



ARTICLE

Comparative Anticancer Mechanisms of *Viscum album* var. *coloratum* Water Extract and Its Lectin on Primary and Metastatic Melanoma Cells

Chang-Eui Hong¹ and Su-Yun Lyu^{2,*}

¹Department of Pharmacy, Sunchon National University, Suncheon, 57922, Republic of Korea

²Institute of Life and Pharmaceutical Sciences, Sunchon National University, Suncheon, 57922, Republic of Korea

*Corresponding Author: Su-Yun Lyu. Email: suyun@scnu.ac.kr

Received: 22 November 2024; Accepted: 05 February 2025; Published: 28 February 2025

ABSTRACT: Objectives: Among cutaneous malignancies, melanoma stands out for its particularly aggressive nature, with therapeutic interventions becoming notably limited once the disease progresses. In this research, we investigate the tumor-suppressing capabilities of water-extracted Korean mistletoe (*Viscum album* var. *coloratum*) and its purified lectin component (*V. album* var. *coloratum* agglutinin, VCA) using two distinct mouse melanoma models: B16BL6 and B16F10 cell lines. **Methods:** The impact of water extract and VCA treatments on melanoma cells was assessed through multiple experimental approaches, examining cellular survival rates, programmed cell death pathways, multicaspase activity, and cell cycle distribution patterns. To elucidate the interconnections among various cellular responses, we employed a suite of statistical techniques encompassing correlation studies, principal component analysis (PCA)-based dimensionality reduction, and dendrogram-based clustering methodologies. **Results:** The water extract exhibited dose-dependent cytotoxicity with IC₅₀ values of 372.3 ± 8.7 µg/mL and 202.5 ± 8.4 µg/mL for B16BL6 and B16F10 cells, respectively. VCA showed more significant effects, with IC₅₀ values of 0.1992 ± 0.0041 and 0.1981 ± 0.0098 µg/mL for B16BL6 and B16F10 cells, respectively. Both agents induced substantial apoptosis with a significant progression from early to late apoptotic stages, reaching up to 59.4% total apoptotic cells for VCA treatment. This was confirmed by strong multicaspase activation, particularly in VCA-treated cells (up to 88.4% caspase-positive cells). The water extract showed modest effects on cell cycle distribution, with increases in G0/G1 phase (74.6%) in B16BL6 cells and S phase (19.2%) in B16F10 cells, while VCA treatment resulted in G2/M phase reduction (10.0%) in B16F10 cells. Correlation analysis revealed strong negative associations between cell viability and caspase activity (r = -0.843 to -0.878), while hierarchical clustering demonstrated distinct response patterns between low and high concentrations of both agents. Effect size analysis confirmed strong treatment impacts on cell viability (d = -5.89 to -6.12) and caspase activation (d = 3.45 to 5.23). **Conclusion:** These findings suggest that Korean mistletoe water extract and its isolated lectin may affect both primary and metastatic melanoma cells through distinct mechanisms, demonstrating particular potency in caspase-dependent apoptosis induction. Our findings establish a robust foundation for developing novel therapeutic interventions derived from natural compounds to combat malignant melanoma with high metastatic potential.

KEYWORDS: Mistletoe; melanoma; apoptosis; cell cycle; caspase; *Viscum album* L. var. *coloratum*

1 Introduction

Despite its lower incidence, cutaneous melanoma represents the deadliest form of skin malignancies, accounting for the majority of skin cancer-related mortality [1]. Global statistics from 2020 documented 324,635 incident cases of melanoma with 57,043 associated fatalities. Contemporary therapeutic advances notwithstanding, patients with metastatic or advanced-stage melanoma face a challenging prognosis,



with five-year survival rates remaining below 22.5% [2]. The pathogenesis of melanoma and its acquired therapeutic resistance stem from multiple molecular alterations. Key signaling cascades in melanoma progression predominantly involve two pathways: the B-Raf Proto-Oncogene, Serine/Threonine Kinase (BRAF) mutation-driven mitogen-activated protein kinase (MAPK) pathway and the phosphoinositide 3-kinase (PI3K)/protein kinase B (AKT) axis, which regulates cellular proliferation and survival mechanisms [3]. These molecular networks significantly influence apoptotic regulation and cell cycle control, representing crucial challenges in melanoma management [4]. Additionally, melanoma cells exhibit altered expression patterns of apoptosis-related proteins, particularly within the B-Cell Lymphoma 2 (Bcl-2) family, potentially conferring resistance to various therapeutic interventions [5]. The B16 murine melanoma cell line and its variants, B16BL6 and B16F10, are widely used to investigate possible treatments for melanoma. Although different, these sublines are known for their high aggressiveness and clear metastatic ability. B16BL6 cells, which were obtained by *in vitro* selection for invasion through a reconstituted basement membrane, show higher lung colonization potential [6]. On the other hand, B16F10 cells, which were derived from the tumor that is selected for the lung colony-forming assay, have high metastatic potential to most organs including the lungs and liver [7]. Because of these differences, they are good models to test the efficacy of potential anticancer drugs against several aspects of melanoma development.

Using these well-established melanoma models, researchers have been actively exploring various therapeutic approaches, with particular interest in natural compounds that could overcome drug resistance. Bioactive compounds from natural sources have emerged as promising candidates for novel cancer therapeutics, potentially circumventing drug resistance mechanisms through their multi-target molecular actions [8]. Among these, Korean mistletoe (*Viscum album* var. *coloratum*), a hemiparasitic plant used in traditional East Asian medicine, has recently gained scientific attention because of its possible anticancer effects [9]. Most of the anticancer properties of Korean mistletoe are due to its bioactive compounds, especially lectins [10]. *V. album* var. *coloratum* agglutinin (VCA) has been identified as one of the most active lectins with cytotoxic effects on several cancer cell lines [11]. Studies on VCA have demonstrated its potential anti-cancer effects in various cancer types. The mechanisms by which VCA exerts its anti-cancer properties are still being explored, however, multiple pathways have been identified. VCA has been demonstrated to cause apoptosis through both intrinsic and extrinsic mechanisms, modify cell cycle progression, and influence various signaling processes involved in the survival and growth of cells [10].

Given that Korean mistletoe and its lectins have shown promising anticancer effects in various cancer types, particularly through modulation of cell death pathways, understanding the fundamental mechanisms of apoptosis in melanoma is crucial. One of the forms of programmed cell death, apoptosis, commonly lacking in melanoma, helps to eradicate cancer cells [12]. The apoptotic cascade encompasses precisely regulated molecular events culminating in the activation of specialized proteolytic enzymes known as caspases, which systematically degrade cellular proteins [13]. The caspase family comprises two distinct functional groups: upstream initiators (caspases 2, 8, 9, and 10) and downstream executioners (caspases 3, 6, and 7) [14]. The activation of initiator caspases occurs through two distinct pathways: the external death receptor-mediated cascade and the internal mitochondrial-dependent pathway. Upon activation, these upstream caspases trigger their downstream counterparts, initiating a proteolytic cascade that induces characteristic cellular modifications indicative of apoptosis [15]. Such cellular transformations encompass chromatin condensation, genomic DNA cleavage, plasma membrane modifications, and ultimate cellular fragmentation into vesicular structures. The progression of apoptotic events can be quantitatively assessed through Annexin V-based detection methods, which identify both early and late-stage apoptotic cells by binding to externalized phosphatidylserine molecules on the cellular surface [16]. At the beginning of the apoptosis, this externalization aids the recognition of the apoptotic cell by phagocytic cells.

While apoptosis is a critical endpoint in cancer cell death, understanding how cell proliferation is regulated through the cell cycle is equally important for developing effective anticancer strategies. Cellular proliferation dynamics are orchestrated through a sequential progression of distinct phases—G1, S, G2, and M—collectively constituting the cell cycle. This intricate process is governed by the coordinated interplay of cyclins, cyclin-dependent kinases (CDKs), and their regulatory inhibitors [17,18]. Contemporary cancer therapeutics frequently target specific components of this cellular machinery. Notable examples include microtubule-stabilizing paclitaxel, which disrupts mitotic progression at the G2/M interface, and the CDK4/6 antagonist palbociclib, which impedes G1 phase transition [19,20]. In the context of melanoma therapeutics, the BRAF inhibitor vemurafenib demonstrates phase-specific activity, inducing G1 phase accumulation specifically in melanoma cells harboring BRAF mutations [21]. Quantitative assessment of cellular DNA content enables the determination of phase distribution patterns and identifies cell cycle perturbations induced by therapeutic interventions [22].

However, while such individual analyses are valuable, they provide only a partial view of cellular responses to anticancer agents. Additionally, analysis of multiple systemic cellular parameters can give a deeper mechanistic understanding of the mode of action of potential therapeutic agents and can exhibit patterns that may not be visible from an individual parameter [23].

This investigation aims to characterize the tumor-suppressive effects of water-extracted Korean mistletoe preparations and its purified lectin component using two distinct murine melanoma models: B16BL6 and B16F10 cell lines. With respect to these compounds, we investigated their effects on cell viability, apoptosis, cell cycle, and multicaspase activity. By comparing the effects of the whole water extract to those of the isolated lectin, we aimed to understand their respective contributions to the observed anticancer activities.

2 Materials and Methods

2.1 Preparation of Korean Mistletoe Water Extract and VCA

The extraction and purification protocols for mistletoe-derived compounds followed previously established methodologies [11]. Plant material was sourced from Korean mistletoe specimens growing on oak trees in Kangwon province, Korea. Following collection, plant tissues underwent mechanical processing to separate leaves, fruit bodies, and stem segments. The processed botanical material underwent mechanical disruption in 10 L of phosphate buffered saline (PBS, pH 7.4, Sigma, P4474, St. Louis, MO, USA) utilizing an industrial-grade extractor (Angelia 8000SS, Angel Life Co., Pocheon, South Korea), followed by centrifugal separation at 12,000 rpm (VS-550, Vision Scientific Co., Daejeon, Korea) for 30 min. The resulting supernatant underwent sequential filtration through a cascade of membrane filters (Cytiva, Marlborough, MA, USA) with decreasing pore sizes: 60, 20, 7.2, 0.45, and 0.22 μm . Extract concentration was determined by calculating the fresh plant material mass per milliliter of the final solution. Lectin quantification in the aqueous extract employed enzyme-linked lectin assay (ELLA) methodology [11]. VCA isolation utilized asialofetuin-Sepharose 4B affinity chromatography. Molecular characterization of VCA, including purity assessment and mass determination, was performed via sodium dodecyl sulfate-polyacrylamide gel electrophoresis (SDS-PAGE, Fig. A1). Protein content was quantified using the bicinchoninic acid (BCA) assay system (Sigma, BCA1).

2.2 Cell Culture and Viability

Metabolic viability was evaluated through tetrazolium salt reduction methodology using 3-(4,5-dimethylthiazol-2-yl)-2,5-diphenyltetrazolium bromide (MTT, Sigma, M5655). Murine melanoma lines (B16BL6 and B16F10) were acquired from Korea Cell Line Bank (Seoul, South Korea). Cells were

maintained in Roswell Park Memorial Institute (RPMI) 1640 medium (Sigma, R8758) enriched with 10% (v/v) fetal bovine serum (FBS, 16000044, Life Technologies, Carlsbad, CA, USA), supplemented with 1% (v/v) non-essential amino acids (Sigma, M7145), 1% (v/v) L-glutamine (Sigma, G7513), and 1% (v/v) penicillin-streptomycin (Sigma, P0781) under standardized culture conditions (37°C, 5% CO₂, humidified environment). Regular screening for mycoplasma contamination was performed using the MycoAlert™ Detection System (Lonza, LT07-318, Basel, Switzerland), with no positive results throughout the experimental period. Culture media was subsequently replaced with fresh preparations containing graduated concentrations of either water-extracted mistletoe preparation (0–1000 µg/mL) or purified VCA (0–1 µg/mL), with appropriate vehicle controls maintained in parallel. Following 48-hour exposure, cellular metabolic activity was assessed by introducing 10 µL of MTT reagent (5 mg/mL in PBS) per well, followed by 4-hour incubation. Post-incubation, media was aspirated and the resultant formazan precipitates were solubilized using 200 µL dimethyl sulfoxide (DMSO, Sigma, D8418) per well. Spectrophotometric measurements were performed at 570 nm with 630 nm reference wavelength using a microplate spectrophotometer (Tecan, Sunrise™, Männedorf, Switzerland). Results were normalized to vehicle-treated controls and expressed as relative viability percentages.

2.3 Apoptosis Analysis

Apoptosis was quantified utilizing fluorescence-based phosphatidylserine detection methodology (Muse™ Annexin V and Dead Cell Assay, EMD Millipore, MCH100105, Billerica, MA, USA). Melanoma cells (B16BL6 and B16F10) were distributed in 6-well culture vessels at 2×10^5 cells per well and maintained overnight to establish adherence. Experimental groups received graduated doses of mistletoe preparations (water extract: 10, 100, and 1000 µg/mL; purified VCA: 0.01, 0.1, and 1 µg/mL) under standard culture conditions (37°C, 5% CO₂) for 48 h. Post-treatment cellular harvesting employed enzymatic dissociation with 0.25% trypsin-EDTA, followed by dual PBS washing cycles and resuspension in culture medium containing 1% FBS to achieve a standardized concentration of 1×10^5 cells/mL. Sample preparation involved combining equal volumes (100 µL) of cell suspension and fluorescent detection reagent (Muse™ Annexin V and Dead Cell Reagent, EMD Millipore, part number 4700–1485) in microcentrifuge vessels. Following gentle homogenization, samples underwent dark incubation at ambient temperature for 20 min. Analysis was performed using microcapillary flow cytometry (Muse™ Cell Analyzer, EMD Millipore, 0500-3115), enabling simultaneous detection of distinct cellular populations: viable cells (dual-negative for Annexin V and 7-AAD), early-stage apoptotic cells (Annexin V-positive/7-AAD-negative), late-stage apoptotic/necrotic cells (dual-positive), and dead cells (Annexin V-negative/7-AAD-positive). Each analysis incorporated 10,000 events, with data processing conducted via specialized software (Muse™ Annexin V and Dead Cell software module, EMD Millipore). Independent experimental replicates (n = 3) were performed, with results presented as mean population percentages ± standard deviation (SD).

2.4 Multicaspase Assay

Caspase activity was monitored using fluorescence-based multi-caspase detection systems (Muse™ MultiCaspase Assay Kit, EMD Millipore, MCH100109). Melanoma cell lines were cultured in 6-well formats at initial densities of 2×10^5 cells per well, allowing attachment over a 24-hour period. Experimental interventions consisted of exposure to either mistletoe aqueous extract (10, 100, and 1000 µg/mL) or purified VCA (0.01, 0.1, and 1 µg/mL) under standardized conditions (37°C, 5% CO₂) for 48 h. Post-exposure processing involved enzymatic cell liberation, sequential buffer washing steps, and cellular suspension preparation in $1 \times$ Assay Buffer to achieve standardized concentrations (1×10^5 cells/mL). Detection protocols utilized a dual-labeling approach, combining 50 µL cellular suspensions with fluorophore-conjugated pan-caspase inhibitor

solution (5 μL Muse™ MultiCaspase reagent, EMD Millipore, part number 4700–1530). The detection system incorporates membrane-permeable fluorescent markers specific for activated caspase enzymes. Sample processing included controlled temperature incubation (37°C, 5% CO₂, 30 min) followed by supplementation with cellular integrity marker (150 μL Muse™ Caspase 7-AAD solution, EMD Millipore, part number 4700–1510). Following brief equilibration at ambient temperature (5 min), samples underwent microcapillary flow cytometric analysis (Muse™ Cell Analyzer, EMD Millipore, 0500–3115). This methodology enabled simultaneous discrimination of four distinct cellular populations: non-apoptotic viable cells (dual-negative), early-stage apoptotic cells (caspase-positive/7-AAD-negative), late-stage apoptotic cells (dual-positive), and non-apoptotic dead cells (caspase-negative/7-AAD-positive). Analysis parameters included the acquisition of 10,000 events per sample, with data processing through specialized analytical software (Muse™ Multi-Caspase module, EMD Millipore). Experimental validation incorporated three independent replicates, with results expressed as population distribution percentages \pm SD.

2.5 Cell Cycle Analysis

Cellular DNA content distribution patterns were evaluated using fluorescence-based cell cycle analysis methodology (Muse™ Cell Cycle Kit, EMD Millipore, MCH100106). Melanoma cells were distributed in multi-well culture vessels at predetermined densities (2×10^5 cells/well) and maintained for 24 h to establish adherence. Experimental interventions comprised exposure to mistletoe-derived preparations (aqueous extract: 10, 100, and 1000 $\mu\text{g}/\text{mL}$; purified VCA: 0.01, 0.1, and 1 $\mu\text{g}/\text{mL}$) under standardized conditions (37°C, 5% CO₂) for 48 h. Post-treatment processing involved enzymatic dissociation, sequential buffer equilibration steps, and cellular fixation using a pre-chilled 70% ethanol solution. The fixation protocol employed gradual cellular suspension introduction into the ethanol medium under continuous vortex agitation. Fixed specimens underwent cold storage (–20°C) for a minimum 3-hour duration prior to analysis. Sample preparation for analysis included dual washing cycles for ethanol removal followed by chromatin staining using a proprietary reagent system (Muse™ Cell Cycle Reagent, EMD Millipore, part number 4700–1495) containing both propidium iodide and ribonuclease A. Following dark incubation at ambient temperature (30 min), samples underwent microcapillary flow cytometric analysis (Muse™ Cell Analyzer, EMD Millipore, 0500–3115). Phase distribution analysis (G0/G1, S, and G2/M) utilized DNA content quantification based on propidium iodide fluorescence intensity measurements. Each analysis incorporated 10,000 discrete events, with data processing conducted through specialized analytical software (Muse™ Cell Cycle module, EMD Millipore). Experimental validation included three independent replicates, with results expressed as mean phase distribution percentages \pm SD.

2.6 Heatmap Analysis

The effects of treatments on cellular parameters were analyzed using heatmap visualization. For each parameter, the fold change relative to control was calculated using the formula: $\log_2(\text{treated}/\text{control})$. For concentrations between measured data points, values were calculated using linear interpolation from adjacent concentrations. The resulting values were visualized as a heatmap where negative values (decreased compared to control) were shown in blue and positive values (increased compared to control) were shown in red, with color intensity corresponding to the magnitude of change ranging from –5 to +5. This analysis was performed using Microsoft Excel (version 2019, Microsoft Corporation, Redmond, WA, USA).

2.7 Principal Component Analysis (PCA)

Multiparametric data analysis was performed using principal component analysis. Ten cellular parameters were analyzed: cell viability, early apoptosis, late apoptosis, total apoptotic cells, caspase-positive cells,

caspase-positive/dead cells, total caspase activity, and cell cycle distribution (G0/G1, S, and G2/M phases). Data were standardized prior to analysis. PCA was conducted using Microsoft Excel with XLSTAT add-in (Addinsoft, Paris, France). The first two principal components (PC1 and PC2) were selected based on their eigenvalues and cumulative explained variance.

2.8 Correlation Analysis of Cellular Parameters

Correlations between cellular parameters were analyzed using Pearson's correlation coefficient (r). The correlation matrices were generated using Microsoft Excel (version 2019, Microsoft Corporation). Correlation coefficients were calculated using the built-in CORREL function, and the resulting matrices were visualized as heatmaps using conditional formatting. The strength and statistical significance of correlations were evaluated according to standard criteria where $|r| > 0.7$ indicates a strong correlation, $0.5 < |r| < 0.7$ indicates a moderate correlation, and $|r| < 0.5$ indicates a weak correlation [24].

2.9 Hierarchical Clustering Analysis

Multiparametric hierarchical clustering analysis was performed using PAST software version 4.17 (University of Oslo, Problemvein, Oslo, Norway). The analysis included 10 cellular parameters: cell viability, early apoptosis, late apoptosis, total apoptotic cells, caspase+, caspase+/dead cells, total caspase, and cell cycle distribution (G0/G1, S, and G2/M phases). Euclidean distance was used as the similarity measure, and the UPGMA (Unweighted Pair Group Method with Arithmetic Mean) algorithm was applied for clustering. The resulting dendrogram was visualized with cell line-specific color coding (B16BL6: blue, B16F10: red, connecting branches: purple) to highlight cell line-specific and shared response patterns.

2.10 Integration Analysis of Cell Cycle Arrest and Apoptosis

The relationship between cell cycle arrest and apoptosis was analyzed by integrating data from cell viability (MTT assay), cell cycle analysis (propidium iodide staining), and apoptosis detection (Annexin V/7-AAD staining). Growth inhibition rate was calculated as $(100 - \text{cell viability})\%$. The data were visualized using bubble charts where the X -axis represents the G0/G1 phase (%), the Y -axis represents total apoptotic cells (%), and the bubble size indicates growth inhibition rate.

2.11 Effect Size Analysis

Effect sizes were calculated using Cohen's d statistic to quantify the magnitude of treatment effects. Cohen's d was computed as the difference between treatment and control means divided by the pooled standard deviation: $d = (M1 - M2)/\sigma_{\text{pooled}}$, where $\sigma_{\text{pooled}} = \sqrt{[(\sigma_1^2 + \sigma_2^2)/2]}$. The 95% confidence intervals were calculated using the standard error of the effect size. Effect sizes were interpreted using Cohen's conventional criteria: small (0.2), medium (0.5), and large (0.8) effects.

2.12 Statistical Analysis

All experiments were performed in triplicate and data are presented as mean \pm SD. For the MTT assay, IC_{50} values were calculated using nonlinear regression analysis with GraphPad Prism version 8.0 (GraphPad Software, San Diego, CA, USA). For flow cytometry experiments, a minimum of 10,000 events were analyzed for each sample. Statistical significance was determined by one-way ANOVA followed by Dunnett's multiple comparison test. p values less than 0.05 were considered statistically significant.

3 Results

3.1 Cytotoxic Effects

The cytotoxicity of Korean mistletoe water extract and VCA on B16BL6 and B16F10 melanoma cells was assessed by MTT assay. Both cell lines were exposed to the water extract at 0–1000 $\mu\text{g}/\text{mL}$ and VCA at 0–1 $\mu\text{g}/\text{mL}$ for 48 h. The water extract exerted a dose-dependent cytotoxic effect on both B16BL6 and B16F10 cell lines (Fig. 1A). In B16BL6 cells, cell viability reduced to $91.86 \pm 8.1\%$ at 125 $\mu\text{g}/\text{mL}$ ($p < 0.05$), $67.47 \pm 3.0\%$ at 250 $\mu\text{g}/\text{mL}$ ($p < 0.01$), and $7.73 \pm 2.1\%$ at 1000 $\mu\text{g}/\text{mL}$ ($p < 0.001$), compared to the untreated control. B16F10 cells also exhibited a similar trend as the cell viability reduced to $83.1 \pm 1.1\%$ at 125 $\mu\text{g}/\text{mL}$ ($p < 0.05$), $35.0 \pm 1.1\%$ at 250 $\mu\text{g}/\text{mL}$ ($p < 0.01$), and $3.2 \pm 0.1\%$ at 1000 $\mu\text{g}/\text{mL}$ ($p < 0.001$), compared to the untreated control. IC_{50} values for the water extract were estimated to be $372.3 \pm 8.7 \mu\text{g}/\text{mL}$ for B16BL6 cells and $202.5 \pm 8.4 \mu\text{g}/\text{mL}$ for B16F10 cells. VCA treatment also led to a dose-dependent reduction in cell viability for both the cell lines (Fig. 1B). For B16BL6 cells, cell viability was reduced to $34.5 \pm 3.0\%$ at 0.25 $\mu\text{g}/\text{mL}$ ($p < 0.01$) and $3.6 \pm 0.9\%$ at 1 $\mu\text{g}/\text{mL}$ ($p < 0.001$), compared to the untreated control. B16F10 cells exhibited decreases in viability to $83.1 \pm 1.2\%$ at 0.125 $\mu\text{g}/\text{mL}$ ($p < 0.05$), $35.0 \pm 1.2\%$ at 0.25 $\mu\text{g}/\text{mL}$ ($p < 0.01$), and $3.2 \pm 0.1\%$ at 1 $\mu\text{g}/\text{mL}$ ($p < 0.001$), compared to the untreated control. IC_{50} values for VCA were determined to be $0.1985 \pm 0.0039 \mu\text{g}/\text{mL}$ for B16BL6 cells and $0.1972 \pm 0.0093 \mu\text{g}/\text{mL}$ for B16F10 cells.

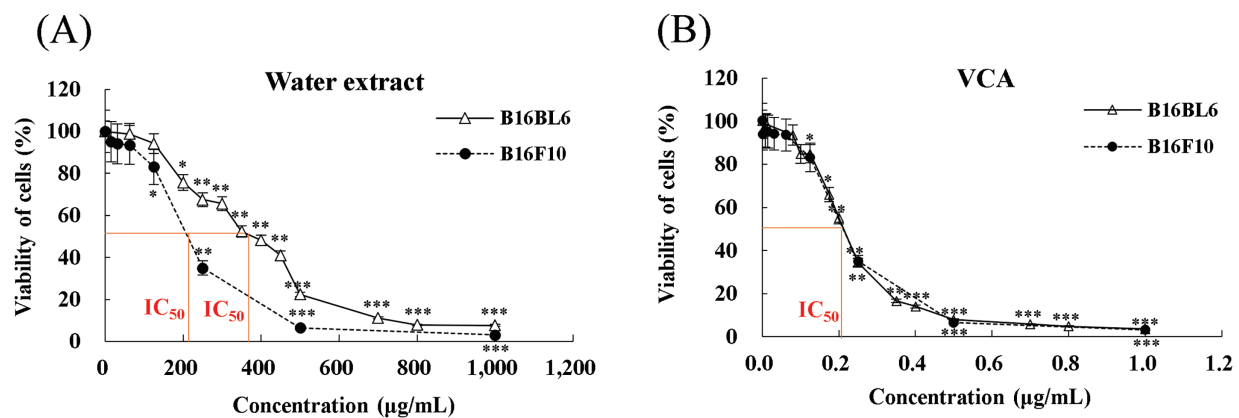


Figure 1: Effects of Korean mistletoe water extract and its lectin (*Viscum album* var. *coloratum* agglutinin, VCA) on melanoma cell viability. (A) B16BL6 and B16F10 cells were treated with various concentrations of water extract (0–1000 $\mu\text{g}/\text{mL}$) for 48 h. (B) Cells were treated with various concentrations of VCA (0–1 $\mu\text{g}/\text{mL}$) for 48 h. Cell viability was assessed using an MTT assay. Data are presented as mean \pm SD from three independent experiments. Statistical significance was determined by 1 one-way ANOVA followed by Dunnett's multiple comparison test (* $p < 0.05$, ** $p < 0.01$, *** $p < 0.001$ vs. control group)

3.2 Apoptosis Induction

The water extract caused a dose-dependent increase in the apoptotic cells in B16BL6 cells (Fig. 2A and B). The percentage of total apoptotic cells was raised from 19.0% in untreated controls to 30.1% ($p < 0.05$), 40.1% ($p < 0.01$), and 42.4% ($p < 0.001$) at 10, 100, and 1000 $\mu\text{g}/\text{mL}$, respectively. At the same time, the percentage of live cells was significantly reduced from 72.75% in controls to 56.8% ($p < 0.05$), 46.9% ($p < 0.01$), and 43.4% ($p < 0.001$) at the corresponding concentrations (data not shown).

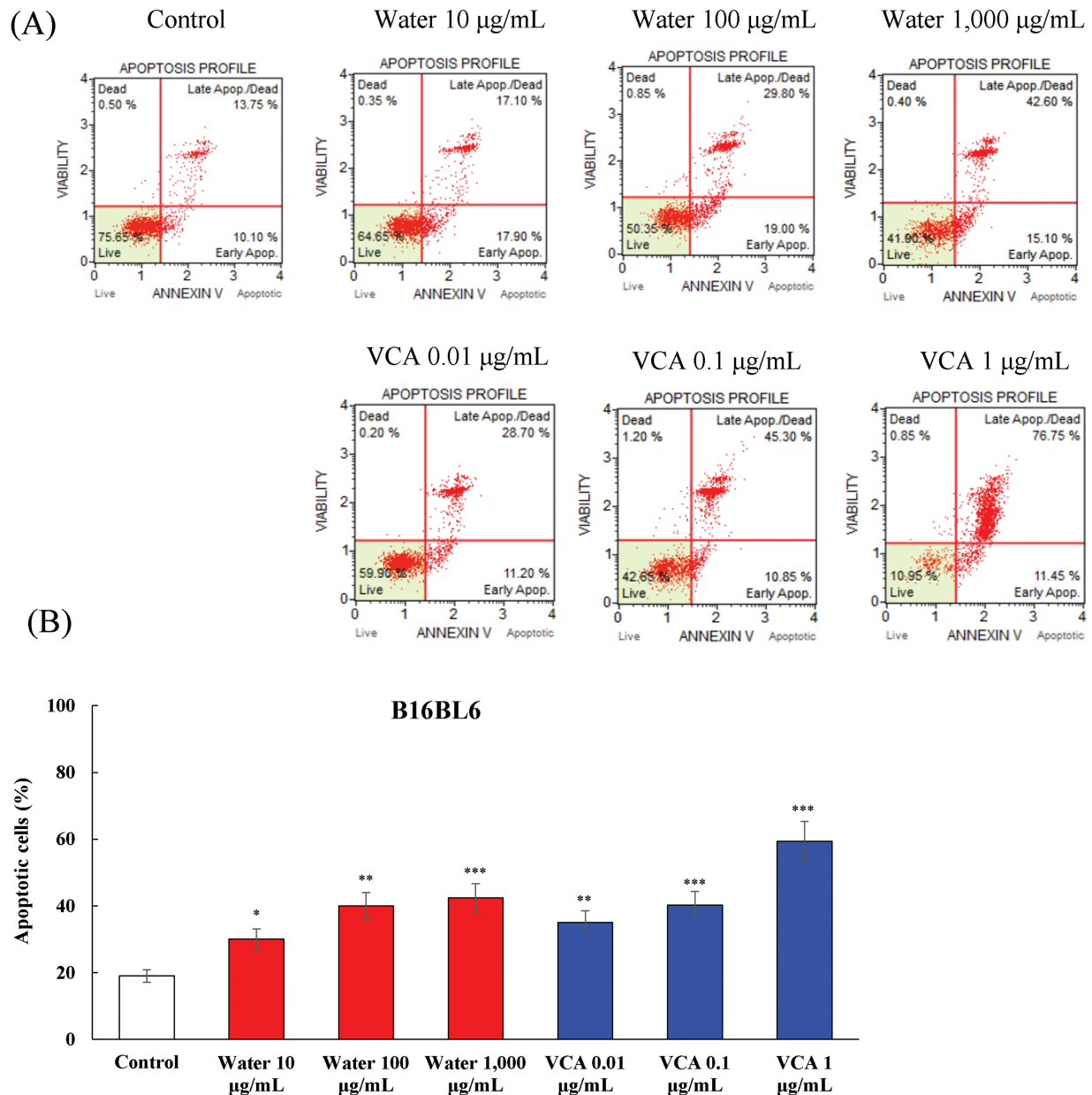


Figure 2: Analysis of apoptosis induction by water extract and its lectin (*Viscum album* var. *coloratum* agglutinin, VCA) in B16BL6 cells. Cells were treated with indicated concentrations (water extract: 0–1000 µg/mL; VCA: 0–1 µg/mL) for 48 h and analyzed by flow cytometry using Annexin V and 7-AAD double staining. The percentages of live cells (Annexin V-/7-AAD-), early apoptotic cells (Annexin V+/7-AAD-), late apoptotic/dead cells (Annexin V+/7-AAD+), and dead cells (Annexin V-/7-AAD+) were quantified. (A) Representative flow cytometry plots are shown. (B) Quantification of total apoptotic cell populations. Data are presented as mean ± SD from two independent experiments. Statistical significance was determined by one-way ANOVA followed by Dunnett's multiple comparison test (* $p < 0.05$, ** $p < 0.01$, *** $p < 0.001$ vs. the control group)

VCA treatment showed a more significant level of apoptosis in B16BL6 cells as compared to the control. The percentage of total apoptotic cells increased from 19.0% in controls to 35.1% ($p < 0.01$), 40.3% ($p < 0.001$), and 59.4% ($p < 0.001$) at 0.01, 0.1, and 1 µg/mL VCA, respectively. The live cell population declined in parallel

from 72.8% in controls to 54.5% ($p < 0.01$), 46.6% ($p < 0.001$), and 17.35% ($p < 0.001$) at these concentrations (data not shown). B16F10 cells also showed the same pattern of apoptosis induction (Fig. 3A and B). Water extract treatment increased the total apoptotic cell population from 14.4% in controls to 27.2% ($p < 0.05$) and 62.0% ($p < 0.001$) at 100 and 1000 $\mu\text{g/mL}$, respectively. The percentage of live cells decreased from 77.2% to 58.7% ($p < 0.05$), and 6.7% ($p < 0.001$) at these concentrations (data not shown). The total apoptotic cell percentages of B16F10 cells treated with VCA were 30.7% ($p < 0.05$), 38.5% ($p < 0.01$), and 57.8% ($p < 0.001$) at 0.01, 0.1, and 1 $\mu\text{g/mL}$, respectively. Likewise, the live cell population reduced from 77.2% to 68.7%, 60.7% ($p < 0.01$), and 41.4% ($p < 0.001$) at the highest concentration (data not shown). The two cell lines showed increased progression from early to late apoptotic stages with increasing concentrations. For B16BL6 cells treated with 1000 $\mu\text{g/mL}$ water extract, the late apoptotic population was 39.3% ($p < 0.01$) compared to 16.6% ($p < 0.05$) early apoptotic cells. Similarly, 1 $\mu\text{g/mL}$ VCA treatment resulted in 69.0% ($p < 0.001$) late apoptotic cells vs. 12.5% ($p < 0.05$) early apoptotic cells. B16F10 cells demonstrated a similar trend, with 1000 $\mu\text{g/mL}$ water extract inducing 65.0% ($p < 0.001$) late apoptotic cells vs. 28.0% ($p < 0.01$) early apoptotic cells, and 1 $\mu\text{g/mL}$ VCA resulting in 48.1% ($p < 0.001$) late apoptotic cells compared to 9.8% ($p < 0.05$) early apoptotic cells (data not shown).

3.3 Multicaspase Activation

The levels of multiple caspases in B16BL6 and B16F10 melanoma cells treated with Korean mistletoe water extract and VCA were determined by flow cytometry-based multicaspase assay. This analysis distinguished four cellular populations: live cells (caspase-negative), caspase-positive cells, caspase-positive/dead cells, and necrotic cells. The water extract caused a dose-dependent activation of caspase in B16BL6 cells (Fig. 4A and B). The percentage of total caspase-positive cells increased from 9.2% in untreated controls to 17.8% ($p < 0.05$), and 23.7% ($p < 0.01$) at 100 and 1000 $\mu\text{g/mL}$, respectively. At the same time, the live cell population reduced from 90.4% to 81.5% ($p < 0.05$), and 75.3% ($p < 0.01$) at these concentrations (data not shown). VCA also led to a higher level of caspase activation in B16BL6 cells as compared to the water extract. The percentage of total caspase-positive cells increased significantly from 9.2% in controls to 17.0% ($p < 0.05$), 30.2% ($p < 0.01$), and 88.4% ($p < 0.001$) at 0.01, 0.1, and 1 $\mu\text{g/mL}$ of VCA, respectively. This was accompanied by a significant decrease in live cells, from 90.4% to 82.2% ($p < 0.05$), 69.4% ($p < 0.01$), and 12.9% ($p < 0.001$) at these concentrations (data not shown).

Caspase activation was also assessed in B16F10 cells, and the results showed a similar trend with some differences in cell sensitivity (Fig. 5A and B). Water extract treatment increased the total caspase-positive population from 10.1% in controls to 29.1% ($p < 0.05$), 27.3% ($p < 0.05$), and 40.7% ($p < 0.001$) at 10, 100, and 1000 $\mu\text{g/mL}$, respectively. The live cell fraction correspondingly decreased from 88.9% to 69.5% ($p < 0.05$), 72.0% ($p < 0.05$), and 58.1% ($p < 0.001$) at the highest concentration (data not shown). Also, VCA treatment of B16F10 cells led to a significant increase in caspase activity. The total caspase-positive cell population increased from 10.1% to 28.9% ($p < 0.05$), 30.0% ($p < 0.05$), and 70.0% ($p < 0.001$) at 0.01, 0.1, and 1 $\mu\text{g/mL}$ of VCA, respectively. This increase was associated with the decrease in live cells from 88.9% to 69.8% ($p < 0.05$), 68.7% ($p < 0.05$), and 29.6% ($p < 0.001$) at the highest VCA concentration (data not shown).

A shift from caspase-positive to caspase-positive/dead cells was observed with increasing concentrations. In B16F10 cells treated with 1000 $\mu\text{g/mL}$ water extract, caspase-positive/dead cells were 30.3% ($p < 0.01$) while caspase-positive cells were 10.4% ($p < 0.05$). Similarly, 1 $\mu\text{g/mL}$ VCA treatment resulted in 47.4% ($p < 0.001$) caspase-positive/dead cells compared to 22.6% ($p < 0.01$) caspase-positive cells. B16F10 cells exhibited a similar pattern, with 1000 $\mu\text{g/mL}$ water extract inducing 30.3% ($p < 0.01$) caspase-positive/dead cells vs. 10.4% ($p < 0.05$) caspase-positive cells, and 1 $\mu\text{g/mL}$ VCA treatment resulting in 47.4% ($p < 0.001$) caspase-positive/dead cells compared to 22.6% ($p < 0.01$) caspase-positive cells (data not shown).

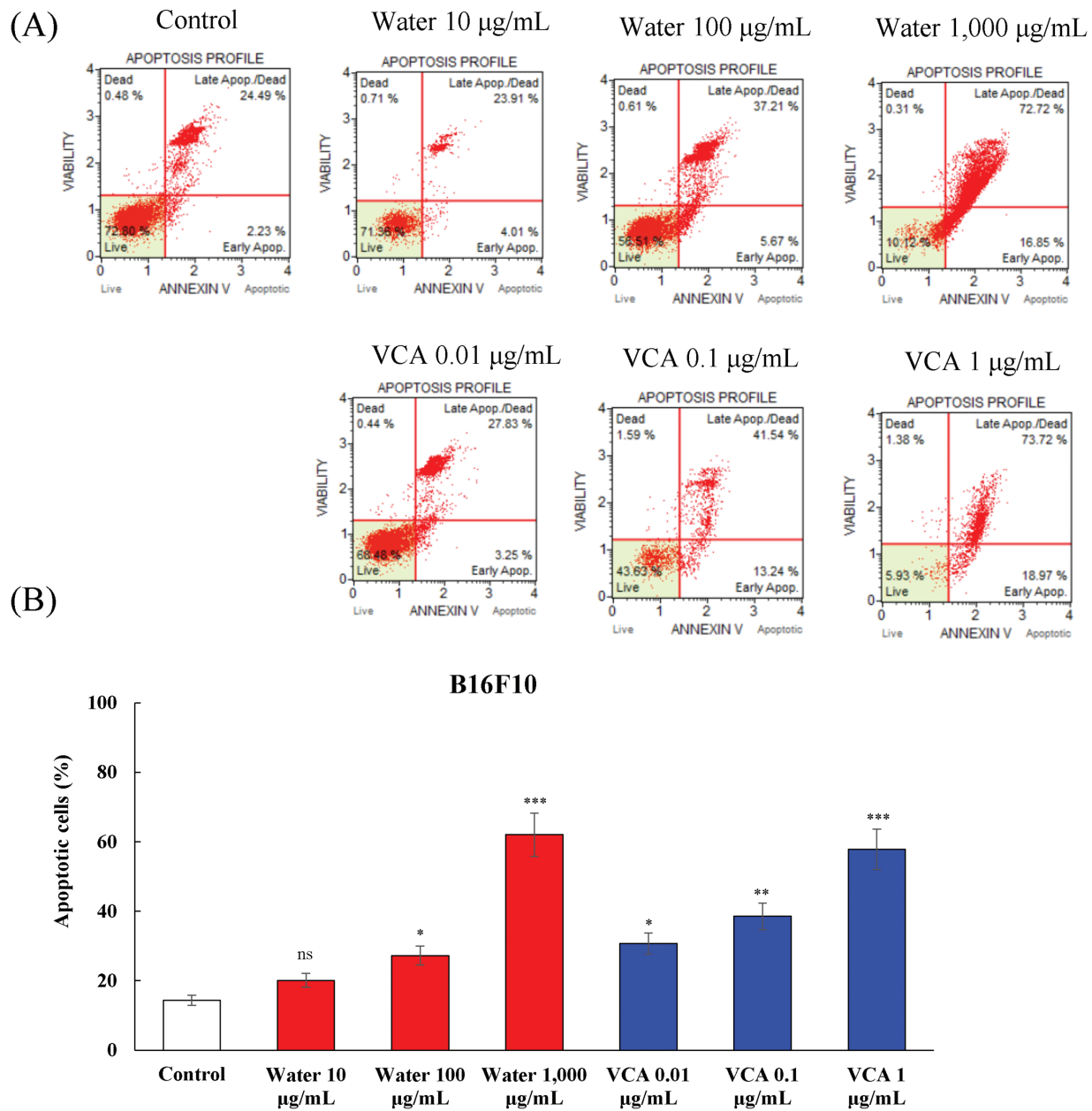


Figure 3: Analysis of apoptosis induction by water extract and its lectin (*Viscum album* var. *coloratum* agglutinin, VCA) in B16F10 cells. Cells were treated with indicated concentrations (water extract: 0–1000 µg/mL; VCA: 0–1 µg/mL) for 48 h and analyzed by flow cytometry using Annexin V and 7-AAD double staining. The percentages of live cells (Annexin V-/7-AAD-), early apoptotic cells (Annexin V+/7-AAD-), late apoptotic/dead cells (Annexin V+/7-AAD+), and dead cells (Annexin V-/7-AAD+) were quantified. (A) Representative flow cytometry plots are shown. (B) Quantification of total apoptotic cell populations. Data are presented as mean ± SD from three independent experiments. Statistical significance was determined by one-way ANOVA followed by Dunnett's multiple comparison test (* $p < 0.05$, ** $p < 0.01$, *** $p < 0.001$ vs. the control group, not significant, ns)

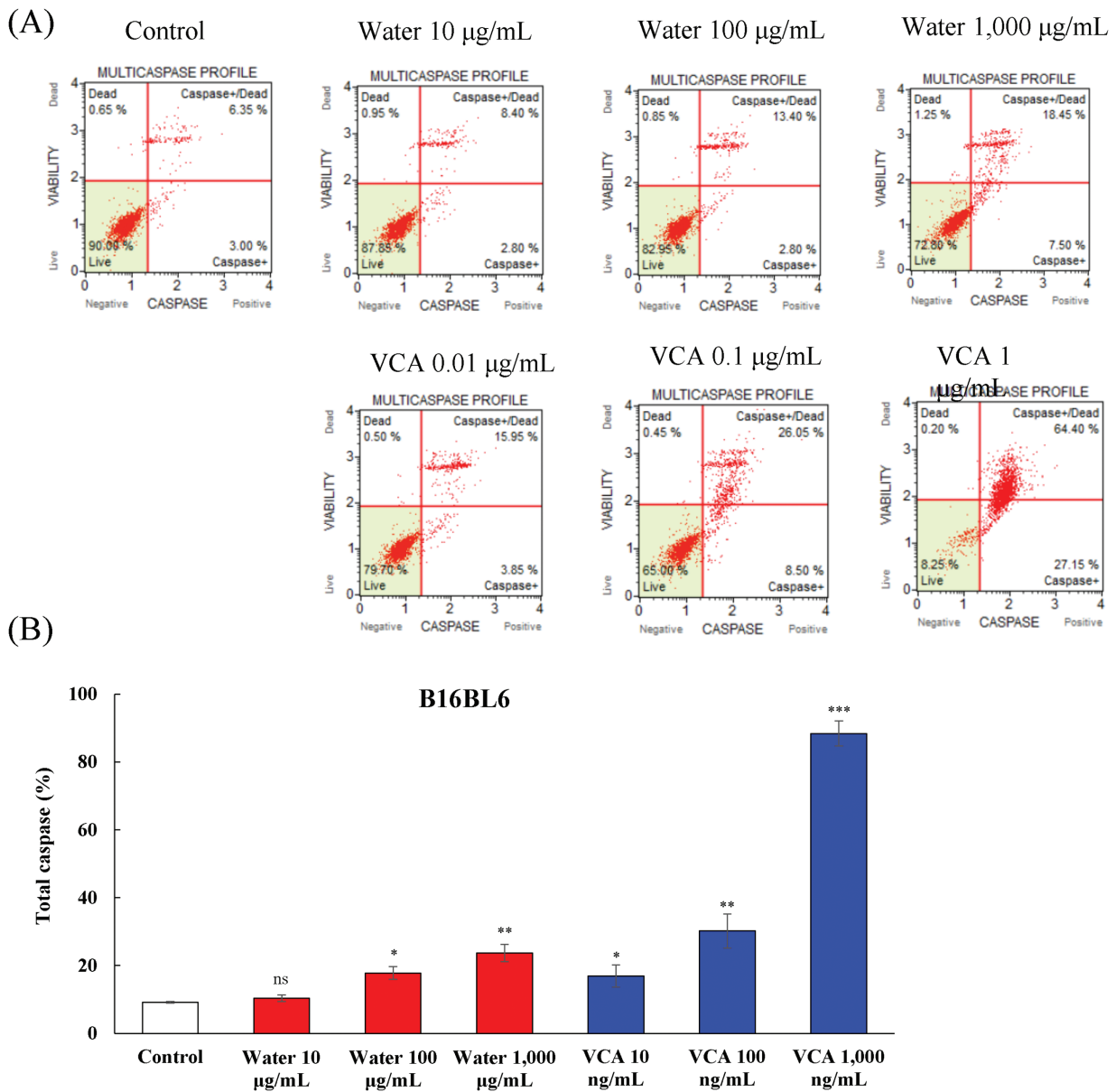


Figure 4: Multicaspase activity analysis in B16BL6 cells treated with water extract and its lectin (*Viscum album* var. *coloratum* agglutinin, VCA). Cells were treated with indicated concentrations (water extract: 0–1000 µg/mL; VCA: 0–1 µg/mL) for 48 h and analyzed by flow cytometry using multicaspase activity assay. The percentages of live cells (caspase-/7-AAD-), caspase-positive cells (caspase+/7-AAD-), caspase-positive/dead cells (caspase+/7-AAD+), and dead cells (caspase-/7-AAD+) were determined. (A) Representative flow cytometry plots are shown. (B) Quantification of total caspase cell populations. Data are presented as mean ± SD from two independent experiments. Statistical significance was determined by one-way ANOVA followed by Dunnett’s multiple comparison test (ns: not significant, * $p < 0.05$, ** $p < 0.01$, *** $p < 0.001$ vs. control group)

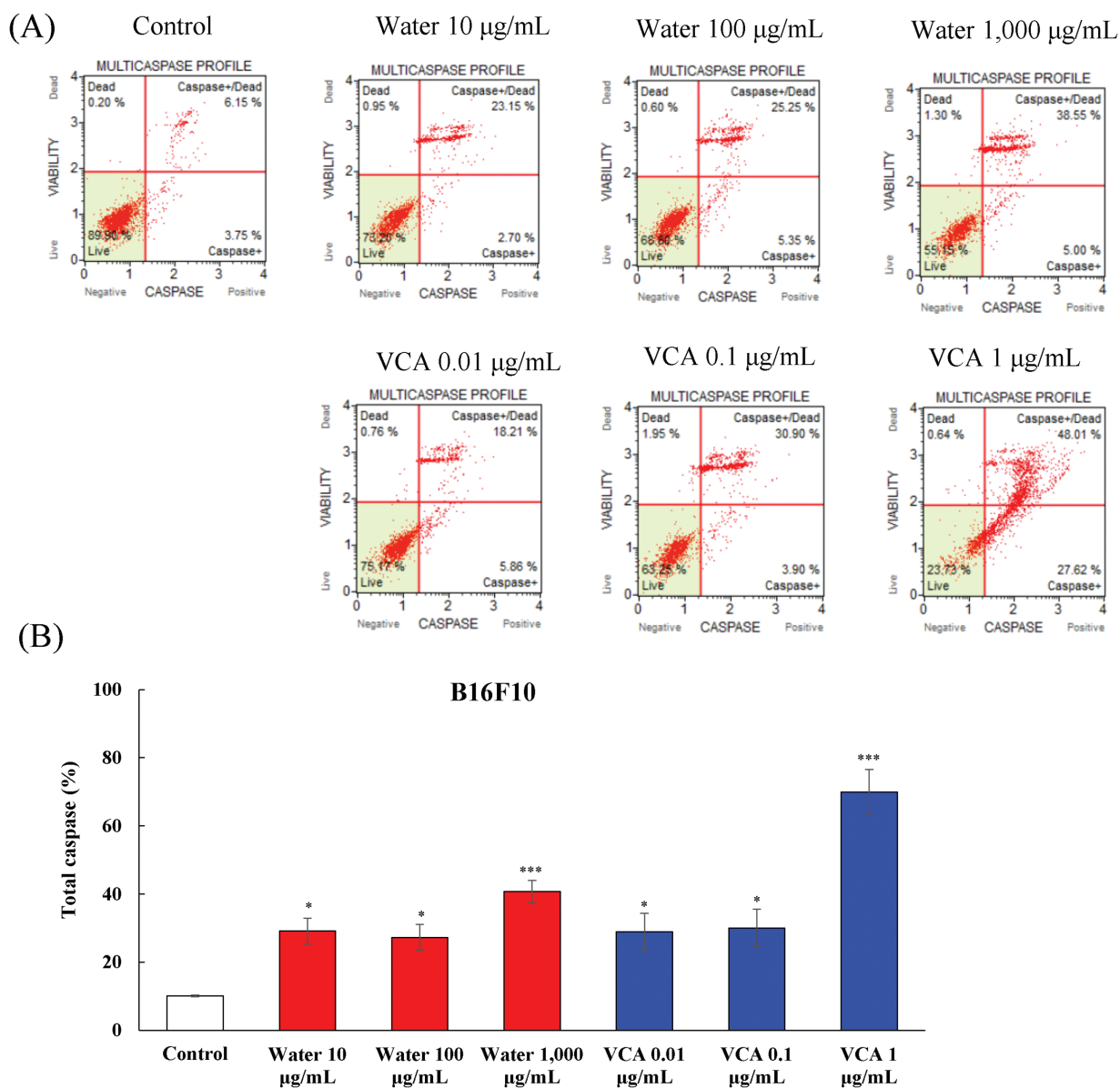


Figure 5: Multicaspase activity analysis in B16F10 cells treated with water extract and its lectin (*Viscum album* var. *coloratum* agglutinin, VCA). Cells were treated with indicated concentrations (water extract: 0–1000 $\mu\text{g/mL}$; VCA: 0–1 $\mu\text{g/mL}$) for 48 h and analyzed by flow cytometry using multicaspase activity assay. The percentages of live cells (caspase-/7-AAD-), caspase-positive cells (caspase+/7-AAD-), caspase-positive/dead cells (caspase+/7-AAD+), and dead cells (caspase-/7-AAD+) were determined. (A) Representative flow cytometry plots are shown. (B) Quantification of total caspase cell populations. Data are presented as mean \pm SD from two independent experiments. Statistical significance was determined by one-way ANOVA followed by Dunnett's multiple comparison test (* $p < 0.05$, *** $p < 0.001$ vs. the control group)

3.4 Cell Cycle Modulation

The water extract caused a dose-dependent change in the percentage of cells in the G0/G1 phase of the cell cycle in B16BL6 cells (Fig. 6A and B). The G0/G1 phase population varied from 68.3% in untreated controls to 67.9% (not significant, ns), 68.033% (ns), and 74.6% ($p < 0.05$) at 10, 100, and 1000 $\mu\text{g/mL}$,

respectively. This G0/G1 change was associated with a fluctuation in the S phase fraction which changed from 9.9% to 8.9% (ns), 9.3% (ns), and 6.6% ($p < 0.05$) at these concentrations. VCA had a different effect on B16BL6 cell cycle progression. The treatment led to a change in the G0/G1 population from 68.3% in the control group to 68.6% (ns), 70.3% (ns), and 65.3% (ns) at 0.01, 0.1, and 1 $\mu\text{g/mL}$. The S phase fraction changed from 9.9% to 9.9% (ns), 7.1% (ns), and 12.3% ($p < 0.05$) at these concentrations.

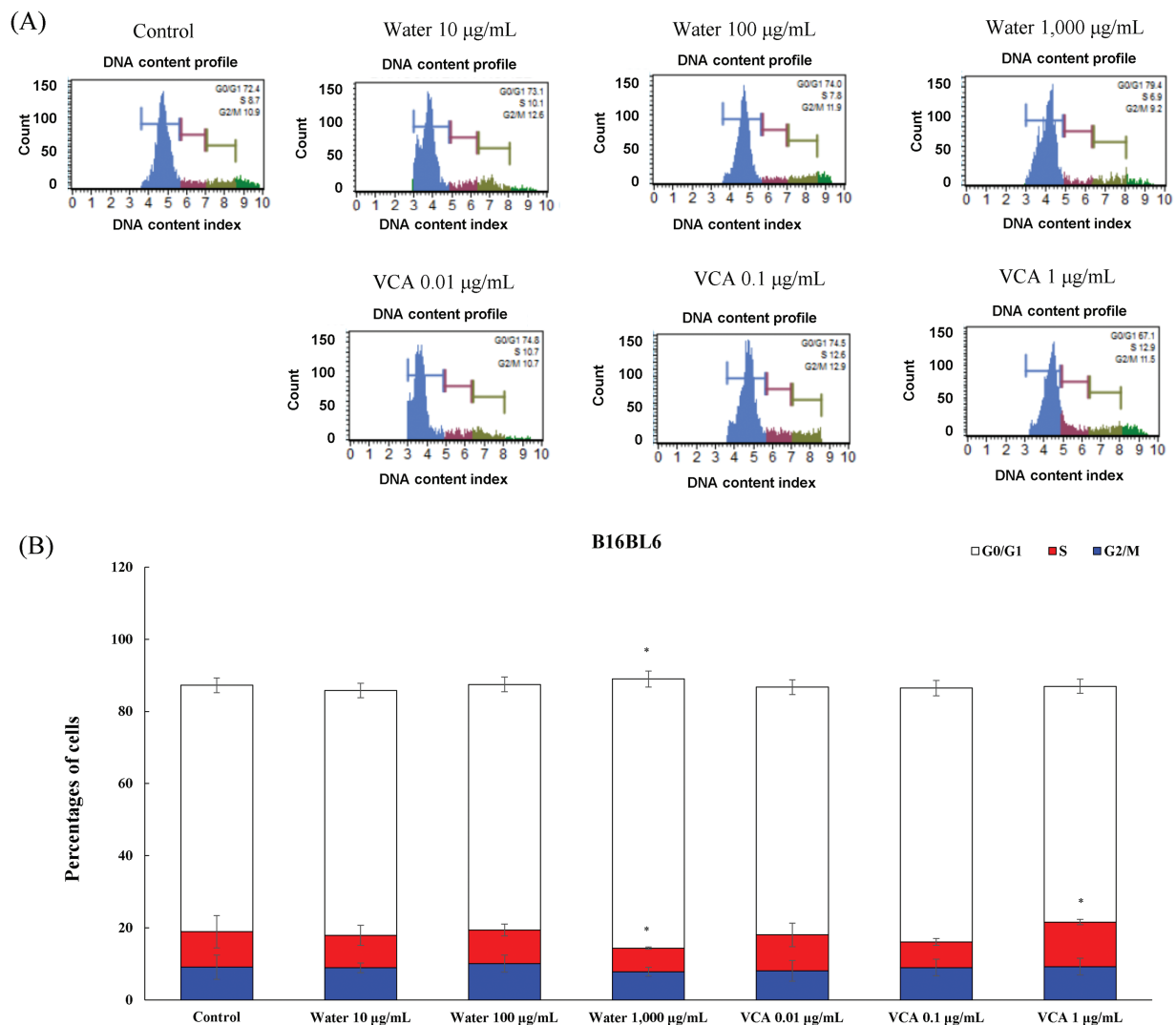


Figure 6: Cell cycle analysis of B16BL6 cells treated with water extract and its lectin (*Viscum album* var. *coloratum* agglutinin, VCA). Cells were treated with indicated concentrations (water extract: 0–1000 $\mu\text{g/mL}$; VCA: 0–1 $\mu\text{g/mL}$) for 48 h and analyzed by flow cytometry following propidium iodide staining. (A) Representative DNA content histograms are shown. (B) Quantification of cells in G0/G1, S, and G2/M phases. Data are presented as mean \pm SD from three independent experiments. Statistical significance was determined by one-way ANOVA followed by Dunnett's multiple comparison test for each cell cycle phase (* $p < 0.05$ vs. respective control group)

The water extract affected B16F10 cells similarly as compared to B16BL6 (Fig. 7A and B). The G0/G1 fraction changed from 66.7% to 65.3% (ns), 66.3% (ns), and 57.1% ($p < 0.05$) at 10, 100, and 1000 $\mu\text{g/mL}$, and significant changes were observed in the S phase, where the cell population changed from 11.7% to 12.9% (ns), 13.2% (ns), and 19.2% ($p < 0.05$) at the highest concentration of the water extract. The VCA treatment

of B16F10 cells induced a change in the G0/G1 population, from 66.7% to 63.4% (ns), 66.1% (ns), and 63.6% (ns) at 0.01, 0.1, and 1 $\mu\text{g/mL}$. This was accompanied by changes in the S phase which changed from 11.7% to 14.5% (ns), 12.7% (ns), and 16.6% ($p < 0.05$). The G2/M phase significantly decreased from 17.8% to 14.9% (ns), 13.1% (ns), and 10.0% ($p < 0.05$) at the highest concentration of VCA.

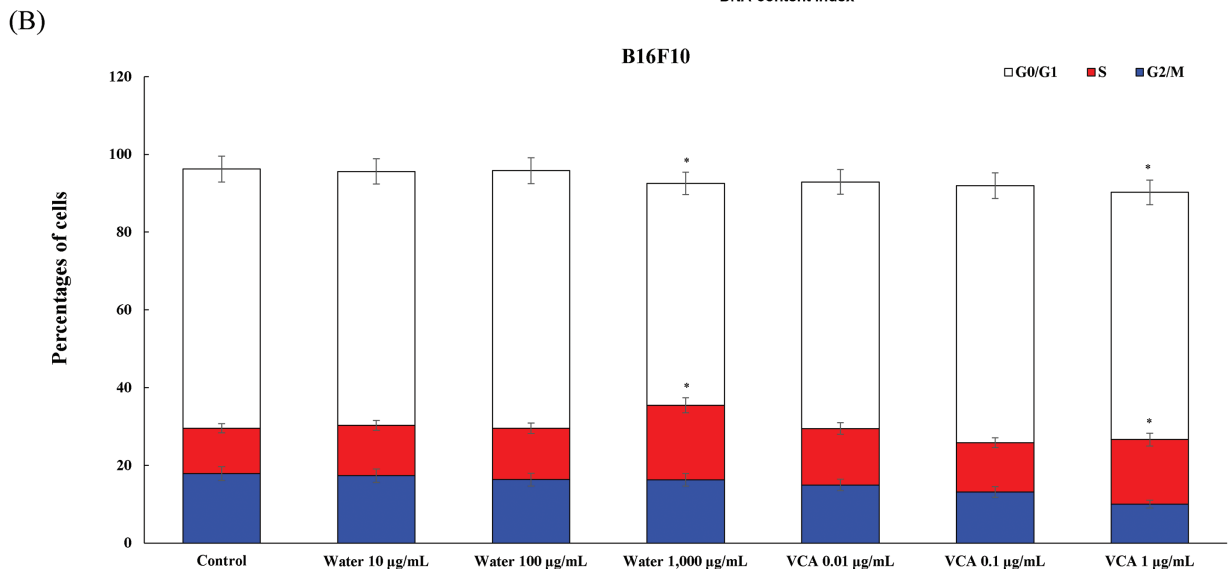
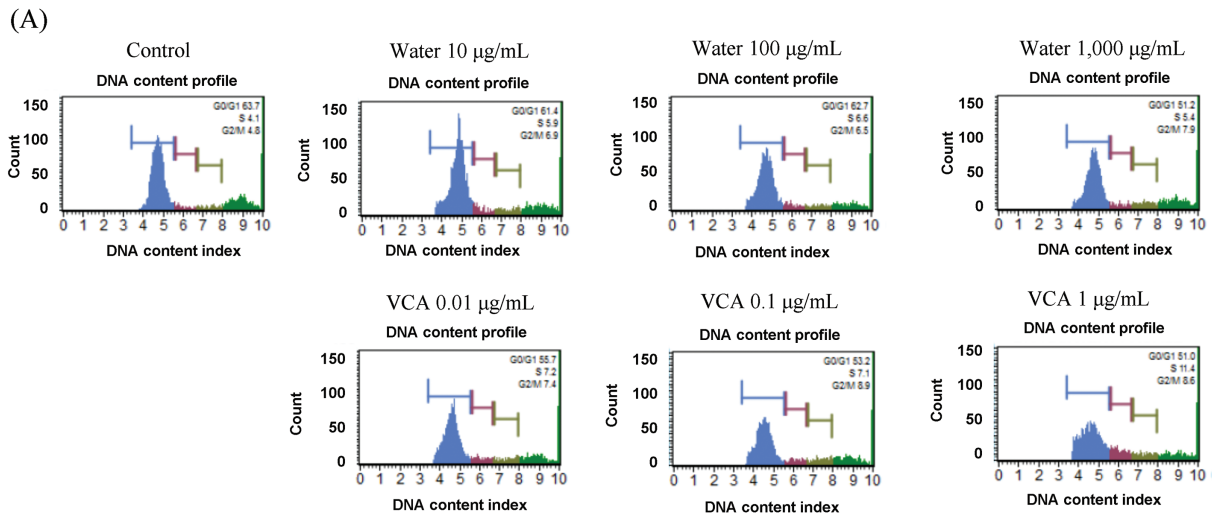


Figure 7: Cell cycle analysis of B16F10 cells treated with water extract and its lectin (*Viscum album* var. *coloratum* agglutinin, VCA). Cells were treated with indicated concentrations (water extract: 0–1000 $\mu\text{g/mL}$; VCA: 0–1 $\mu\text{g/mL}$) for 48 h and analyzed by flow cytometry following propidium iodide staining. (A) Representative DNA content histograms are shown. (B) Quantification of cells in G0/G1, S, and G2/M phases. Data are presented as mean \pm SD from three independent experiments. Statistical significance was determined by one-way ANOVA followed by Dunnett's multiple comparison test for each cell cycle phase ($*p < 0.05$ vs. respective control group)

3.5 Comprehensive Analysis of Treatment Effects Using Heatmap Visualization

To understand the overall patterns of cellular responses to water extract and VCA treatments, we performed a heatmap analysis of all measured parameters (Fig. 8A and B). In B16BL6 cells, VCA at 1 $\mu\text{g/mL}$ showed the most dramatic effect on cell viability (\log_2 fold change: -4.8125) compared to water extract

at 1000 µg/mL (−3.6938). Notably, both treatments showed strong induction of caspase activation, with VCA demonstrating particularly potent effects on total caspase (3.2718) and caspase+/dead cells (3.3181). In B16F10 cells, while the water extract at 1000 µg/mL showed a strong reduction in cell viability (−4.9801), VCA exhibited more moderate effects except at the highest concentration. Interestingly, both cell lines showed minimal changes in cell cycle parameters (generally within ±0.5 log₂ fold change), suggesting that the cytotoxic effects are primarily mediated through apoptotic pathways rather than cell cycle arrest. The analysis revealed that while both agents induced similar patterns of cellular responses, VCA generally showed more potent effects on apoptotic and caspase markers, particularly in B16BL6 cells.

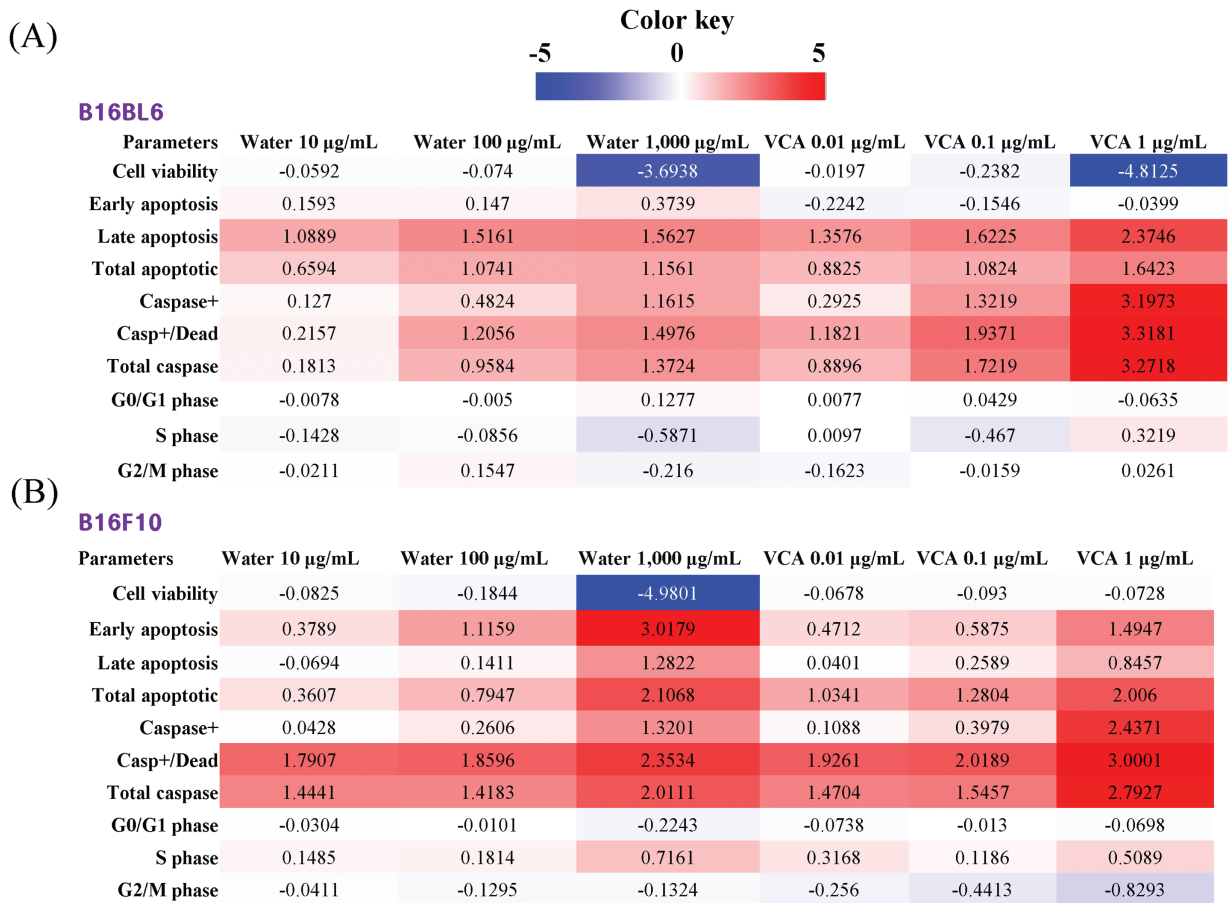


Figure 8: Heatmap analysis of treatment effects on (A) B16BL6 and (B) B16F10 melanoma cells. Changes in cellular parameters in response to water extract of Korean mistletoe and its lectin (*Viscum album* var. *coloratum* agglutinin, VCA) were visualized using heatmaps. Fold changes were calculated as a log₂ ratio of treated vs. control values for each parameter. The color scale represents the magnitude and direction of changes, with red indicating increased values and blue indicating decreased values relative to control. The intensity of colors corresponds to the magnitude of change, ranging from +5 (brightest red) to −5 (brightest blue). Cellular parameters analyzed include cell viability, apoptotic markers (early apoptosis, late apoptosis, total apoptotic cells), caspase activation markers (caspase+, caspase+/dead cells, total caspase), and cell cycle distribution (G0/G1, S, and G2/M phases)

3.6 PCA

To comprehensively understand the differential effects of water extract and VCA on both melanoma cell lines, we performed PCA integrating all measured parameters (Fig. 9). The analysis revealed that PC1 and PC2 explained 58.3% and 24.7% of the total variance, respectively. The PCA plot showed a clear separation between water extract and VCA treatments along PC1, suggesting distinct mechanisms of action. Additionally, the two cell lines clustered separately along PC2, indicating cell line-specific responses to both treatments.

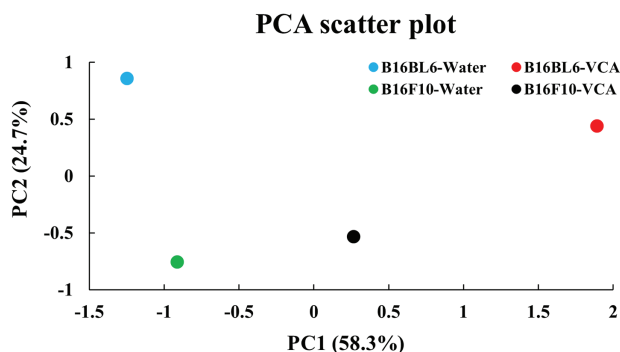


Figure 9: Principal component analysis (PCA) of multiparametric data from B16BL6 and B16F10 cells treated with Korean mistletoe water extract and its lectin (*Viscum album* var. *coloratum* agglutinin, VCA). PCA was performed using ten cellular parameters including cell viability, apoptotic markers (early apoptosis, late apoptosis, total apoptotic cells), caspase activation markers (caspase+, caspase+/dead cells, total caspase), and cell cycle distribution (G0/G1, S, and G2/M phases). PC1 and PC2 represent the first and second principal components explaining 58.3% and 24.7% of the total variance, respectively. Each dot represents a different experimental condition: B16BL6-Water (blue), B16BL6-VCA (red), B16F10-Water (green), and B16F10-VCA (black)

3.7 Correlation Analysis

To better understand the relationships between different cellular parameters, we performed a correlation analysis (Fig. 10A and B). In B16BL6 cells, strong negative correlations were observed between cell viability and caspase activity markers ($r = -0.843$ for total caspase). Total caspase activity showed strong positive correlations with both caspase+/dead cells ($r = 0.998$) and late apoptosis ($r = 0.927$), suggesting coordinated activation of apoptotic pathways. Interestingly, the G0/G1 phase showed a positive correlation with cell viability ($r = 0.877$) but negative correlations with apoptotic markers.

Similar correlation patterns were observed in B16F10 cells, with slightly stronger negative correlations between cell viability and both apoptotic ($r = -0.923$) and caspase markers ($r = -0.878$ for total caspase). However, B16F10 cells showed stronger correlations between early apoptosis and caspase markers ($r = 0.912$) compared to B16BL6 cells, suggesting potential differences in the timing or mechanism of apoptosis activation between the two cell lines.

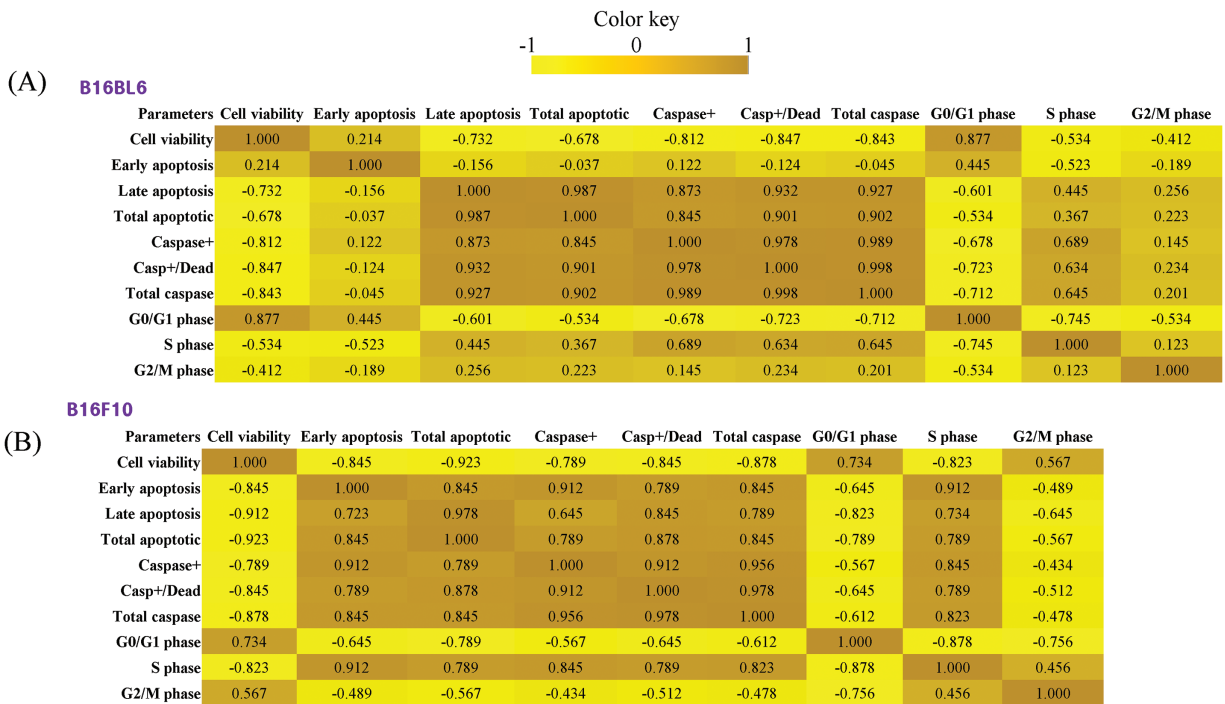


Figure 10: Correlation analysis of cellular parameters in B16BL6 and B16F10 melanoma cells treated with Korean mistletoe water extract and its lectin (*Viscum album* var. *coloratum* agglutinin, VCA). Pearson correlation coefficients were calculated between different cellular parameters including cell viability, apoptotic markers (early apoptosis, late apoptosis, total apoptotic cells), caspase activation markers (caspase+, caspase+/dead cells, total caspase), and cell cycle distribution (G0/G1, S, and G2/M phases). The correlation matrices are visualized as heatmaps where the color intensity represents the strength and direction of correlations (brown: positive correlation, yellow: negative correlation). (A) Correlation matrix for B16BL6 cells. (B) Correlation matrix for B16F10 cells

3.8 Hierarchical Clustering Analysis

Hierarchical clustering analysis revealed distinct treatment response patterns between B16BL6 and B16F10 melanoma cells (Fig. 11). Low and medium concentrations of both water extract and VCA (10–100 µg/mL and 0.01–0.1 µg/mL, respectively) clustered together within each cell line, suggesting cell line-specific responses at these concentrations. However, high concentrations (1000 µg/mL water extract and 1 µg/mL VCA) formed a separate cluster, indicating similar response patterns regardless of the cell line. Within the low/medium concentration clusters, treatments showed dose-dependent clustering patterns, with B16BL6-VCA 0.01 µg/mL and B16BL6-Water 100 µg/mL showing closer relationships compared to their respective lower concentrations.

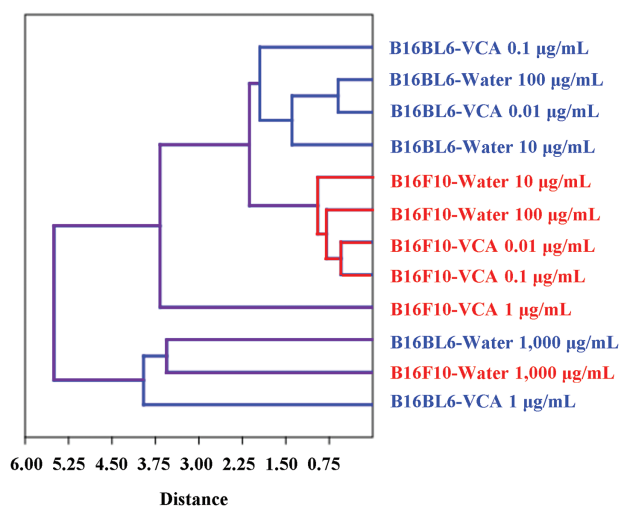


Figure II: Hierarchical clustering analysis of treatment responses in B16BL6 and B16F10 melanoma cells treated with Korean mistletoe water extract and its lectin (*Viscum album* var. *coloratum* agglutinin, VCA). Multiparametric analysis was performed using 10 cellular parameters including cell viability, apoptotic markers, caspase activation markers, and cell cycle distribution. The dendrogram shows the relationship between different treatment conditions, with the distance scale indicating the degree of similarity. Blue branches represent B16BL6-specific clusters, red branches represent B16F10-specific clusters, and purple branches show connections between cell lines. Treatment conditions are labeled as cell line-treatment type-concentration

3.9 Integration Analysis

To understand the relationship between cell cycle arrest and apoptosis induction, we performed an integration analysis incorporating cell viability data (Fig. 12A and B). In B16BL6 cells, water extract treatment showed a concentration-dependent increase in both G0/G1 arrest and apoptosis, with the highest concentration (1000 µg/mL) inducing strong G0/G1 arrest (74.6%) along with significant apoptosis (42.4%) and growth inhibition (92.3%). VCA treatment, particularly at 1 µg/mL, demonstrated potent apoptosis induction (59.4%) with moderate G0/G1 arrest (65.3%) and strong growth inhibition (96.4%). Integration analysis of B16F10 cells revealed distinct mechanisms between water extract and VCA treatments. Water extract at 1000 µg/mL demonstrated potent apoptotic effects (62.03% total apoptotic cells) concurrent with G0/G1 phase reduction to 57.1%, corresponding to 96.83% growth inhibition. VCA at 1 µg/mL induced comparable growth inhibition (96.83%) with 57.83% apoptotic cells while maintaining the G0/G1 phase at 63.6%. At lower concentrations, both agents showed dose-dependent increases in apoptotic populations with minimal effects on G0/G1 distribution. This response pattern differs from B16BL6 cells, where water extract induced G0/G1 accumulation, suggesting cell line-specific differences in cell cycle regulation mechanisms between primary and metastatic melanoma cells.

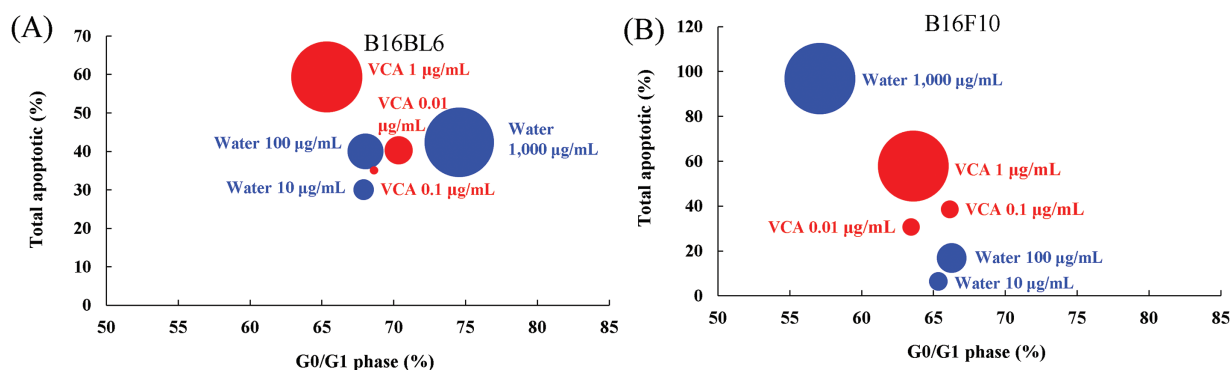


Figure 12: Integration analysis of cell cycle arrest and apoptosis induction in melanoma cells treated with Korean mistletoe water extract and its lectin (*Viscum album* var. *coloratum* agglutinin, VCA). The relationship between G0/G1 phase arrest and total apoptotic cells was visualized using bubble charts where bubble size represents the growth inhibition rate (100-cell viability %). (A) B16BL6 cells and (B) B16F10 cells were treated with various concentrations of water extract (blue bubbles; 10, 100, 1000 µg/mL) or VCA (red bubbles; 0.01, 0.1, 1 µg/mL) for 48 h. Control values were G0/G1: 68.3%, Total apoptotic: 19.0% for B16BL6; G0/G1: 66.7%, Total apoptotic: 14.4% for B16F10. Larger bubbles indicate stronger growth inhibition effects. Data represent the mean values from three independent experiments

3.10 Effect Size Analysis

Effect size analysis revealed strong dose-dependent effects of both water extract and VCA treatments (Fig. 13A–D). The strongest effects were observed in cell viability ($d = -5.89$ to -6.12) and total caspase activation ($d = 3.45$ to 5.23) at the highest concentrations. Both B16BL6 and B16F10 cells showed similar patterns of effect sizes, though B16BL6 cells demonstrated slightly stronger responses to VCA treatment in terms of caspase activation ($d = 5.23$ vs. 4.56). Cell cycle parameters showed moderate effects, with the most pronounced changes in S phase distribution.

4 Discussion

The present study on the antiproliferative and pro-apoptotic activity of Korean mistletoe water extract and its isolated lectin on B16BL6 and B16F10 melanoma cells demonstrated some promising results. The water extract resulted in a highly significant ($p < 0.001$) dose-dependent cell death occurring in the range of 0–1000 µg/mL due to the presence of various bioactive compounds, including lectins, viscotoxins, and polysaccharides [25]. This indicates that whole plant extracts may be useful in cancer treatment as all the parts of the plant may work together to achieve the desired therapeutic effect [26]. Our results show that B16BL6 and B16F10 cells have different sensitivities to the water extract, with IC_{50} of 372.3 ± 8.7 µg/mL and 202.5 ± 8.4 µg/mL for B16BL6 and B16F10 cells, respectively, suggesting that B16F10 cells are significantly more sensitive to the water extract. This variation could be attributed to the different metastatic potential of these cell lines; B16F10 cells may show higher sensitivity despite their ability to colonize multiple organs, while B16BL6 cells, which primarily target the lungs, demonstrate relatively lower sensitivity [6]. Additionally, the variation in response of these cell lines implies that the mistletoe water extract may be affecting pathways related to metastasis. For instance, they could be regulating Epithelial-mesenchymal transition (EMT) markers, such as E-cadherin, vimentin, or matrix metalloproteinases (MMPs) that promote invasion [27]. These effects may also be involved in the other anti-metastatic activities of mistletoe extracts that have been described in some studies [28]. In addition, VCA showed high cytotoxicity at nanogram levels, with statistically significant effects ($p < 0.001$) at higher concentrations, which is consistent with other studies on mistletoe lectins [29]. The IC_{50} values of VCA for the two metastatic melanoma cell lines B16BL6 and

B16F10 were 0.1992 ± 0.0041 and 0.1981 ± 0.0098 $\mu\text{g/mL}$, respectively, which shows that VCA also has a potent antiproliferative activity. Mistletoe lectins have been observed to inhibit the PI3K/AKT/mTOR pathway which is vital for the existence of melanoma cells [30]. Furthermore, the MAPK pathway which is activated in melanoma due to overexpression of BRAF might be another target of these compounds [31]. Additionally, the efficacy of both water extract and VCA suggests they can be utilized for targeting primary tumors and metastatic cells, both of which are critical components in melanoma treatment [32]. Further research is needed, most especially on EMT markers, MMPs, and cell adhesion molecules (CAMs) [33] to investigate the possible anti-metastatic properties of these compounds.

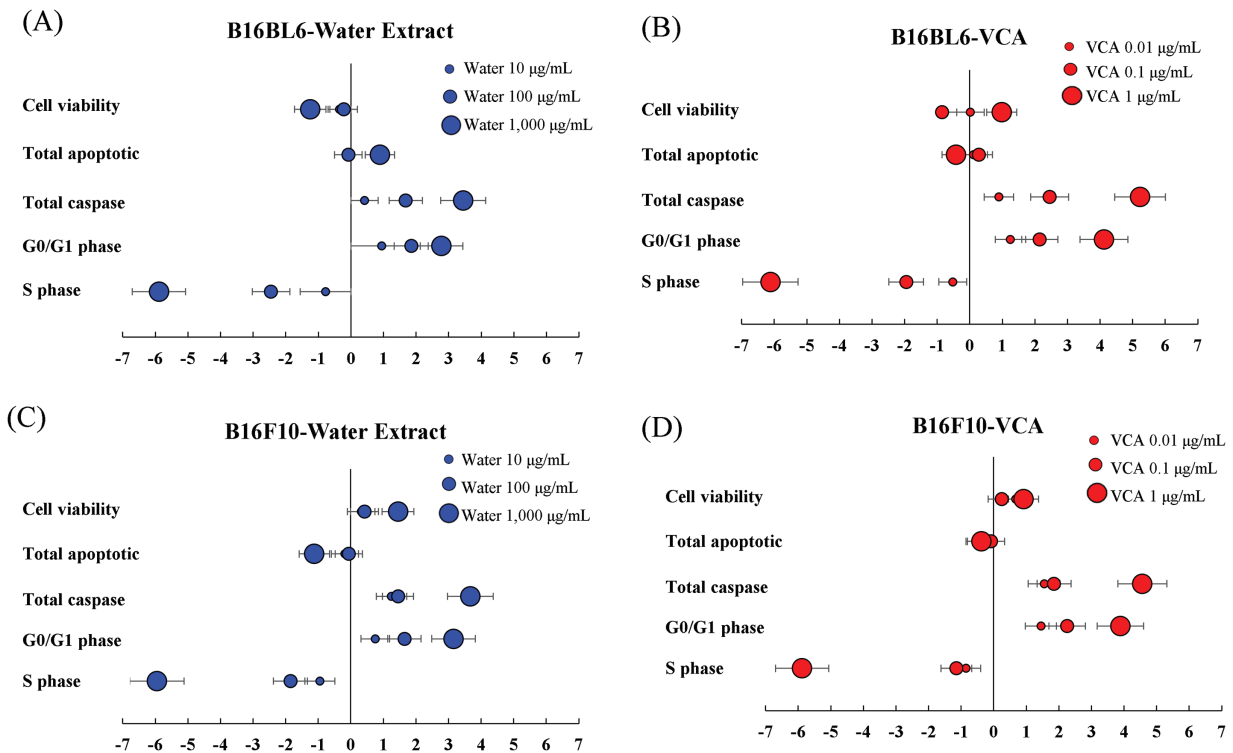


Figure 13: Effect size analysis of Korean mistletoe water extract and its lectin (*Viscum album* var. *coloratum* agglutinin, VCA) treatment on melanoma cells. Effect sizes (Cohen's d) were calculated for multiple cellular parameters including cell viability, apoptotic markers, caspase activation, and cell cycle distribution. (A) B16BL6 cells treated with water extract (10, 100, 1000 $\mu\text{g/mL}$), (B) B16BL6 cells treated with VCA (0.01, 0.1, 1 $\mu\text{g/mL}$), (C) B16F10 cells treated with water extract (10, 100, 1000 $\mu\text{g/mL}$), and (D) B16F10 cells treated with VCA (0.01, 0.1, 1 $\mu\text{g/mL}$) for 48 h. Effect sizes were calculated using pooled standard deviations, and error bars represent 95% confidence intervals. Horizontal reference lines indicate conventional thresholds for small (± 0.2), medium (± 0.5), and large (± 0.8) effects. Negative values indicate a decrease from control, positive values indicate an increase from control

The cell death pathways activated by both the water extract and VCA were elucidated using apoptosis and multicaspase assays. A dose-dependent increase in the apoptotic cells with significant progress from early to late apoptosis was induced by both agents. Exposure of B16BL6 cells to water extract increased total apoptotic cells from 19.0% up to 42.4%, with statistical significance at all concentrations tested ($p < 0.05$ to $p < 0.001$), while VCA showed a more pronounced effect, increasing apoptotic cells to 59.4% ($p < 0.001$) at the highest concentration. Similarly, the total apoptotic population increased to 62.0% ($p < 0.001$) with water extract and 57.8% ($p < 0.001$) with VCA treatment in B16F10 cells. This was further confirmed by the multicaspase assay which showed the significant activation of several caspases at the

same time. The multicaspase data revealed that VCA induced stronger caspase activation than the water extract, particularly in B16BL6 cells where total caspase-positive cells reached 88.4% ($p < 0.001$) compared to 23.7% ($p < 0.01$) with water extract treatment. The pattern of caspase activation observed (increase in both caspase positive and caspase positive/dead cells) indicates the activation of several apoptotic pathways. This suggests that mistletoe water extract and VCA may be affecting multiple molecules. In the intrinsic pathway, they may be affecting the balance between the proteins that cause apoptosis like Bax and Bak, and the proteins that prevent apoptosis like Bcl-2 and Bcl-xL [10]. The extrinsic pathway is likely to be similarly disrupted by these compounds, either by interfering with death receptor signaling, or perhaps by upregulation of death receptors and their ligands [34]. This is useful in melanoma therapy because these tumors usually acquire resistance to apoptosis by different mechanisms. In all treatments and cell lines, a significantly positive association was found between the apoptotic populations and caspase activation. Treatment of VCA at 1 $\mu\text{g}/\text{mL}$ in B16BL6 cells resulted in significant apoptosis (total apoptotic cells: 59.4% ($p < 0.001$)) and substantial caspase activation (total caspase-positive cells: 88.4% ($p < 0.001$)). While these two independent measurements suggest robust cell death signaling, they represent distinct cellular events and cannot be directly compared. Treatment with 1000 $\mu\text{g}/\text{mL}$ of water extract in B16F10 cells also caused significant apoptosis (62.0% of apoptotic cells, $p < 0.001$) and increased caspase activation (40.7% of caspase positive cells, $p < 0.001$). Independent measurements of these results show that the apoptotic pathways are activated, even though the assays represent different dimensions of the cell death process. However, these similar findings observed in multiple assays and also cell lines imply that the cell death we have seen is largely through caspase-dependent apoptotic pathways. Additionally, a dose-dependent increase in apoptotic pathways, with movement from early to late apoptosis and increased caspase activity as the concentration increases, was observed. This is shown by the transition from caspase-positive to caspase-positive/dead cells at higher concentrations of both the water extract and VCA. At 1000 $\mu\text{g}/\text{mL}$, caspase-positive cells increased to 10.4% with caspase-positive/dead cells reaching 30.3% ($p < 0.001$) and the total apoptotic population increased from 14.4% to 62.0% ($p < 0.001$) in B16F10 cells treated with water extract. Kinetics of Annexin V and multicaspase assay indicate that caspase activation and apoptosis induction constitute linked processes. The fact that most of the current targeted therapies for melanoma, for example, BRAF inhibitors, often lead to acquired resistance mediated via activation of other survival pathways [35], suggests using these molecules as adjuvant or alternative therapies to existing therapies since they can circumvent apoptosis resistance mechanisms commonly experienced in melanoma. In particular, the ability to activate multiple caspases can be useful in overcoming the over-expression of anti-apoptotic proteins often seen in melanoma and which contribute to resistance to therapy [36], thus opening the possibility for a multiple-targeted approach to treat this disease.

We further demonstrated that both water extract and VCA possess modest and selective cellular effects on cell cycle distribution. In B16BL6 cells, the water extract induced changes in cell cycle phases at the highest concentration, with a rise in G0/G1 phase (from 68.3% to 74.6%, $p < 0.05$) and at the lowest concentration, an increase in S phase (from 11.7% to 19.2%, $p < 0.05$) in B16F10 cells. These cell type-specific responses were evident in the differential effects of the treatments: water extract significantly increased S phase (to 19.2%, $p < 0.05$) with G0/G1 decrease in B16F10 cells, while its effect on B16BL6 cells was primarily seen as S phase decreased. VCA showed a distinct pattern with a G2/M decrease (to 10.0%, $p < 0.05$) in B16F10 cells. These varied responses suggest that these effects on the cell cycle might be downstream of the primary apoptotic mechanisms, a common pattern for natural anticancer compounds that primarily target apoptotic pathways [37–39]. VCA treatment similarly resulted in changes, showing a statistically significant increase in the S phase population in B16BL6 cells (from 9.9% to 12.3%, $p < 0.05$) and a decrease in G2/M phase in B16F10 cells (from 17.8% to 10.0%, $p < 0.05$). While the cell cycle effects were less pronounced than the

apoptotic responses, the observed changes in S phase population—particularly the decrease to 6.6% ($p < 0.05$) with water extract and increase to 12.3% ($p < 0.05$) with VCA at highest concentrations—suggest that these agents might have distinct effects on cell cycle regulation in B16BL6 cells. However, these cell cycle changes appear to be secondary to the primary apoptotic mechanisms [40]. Based on this interpretation of cell cycle effects, we propose that the predominant anticancer activity of these compounds is due to direct activation of apoptotic pathways, rather than cell cycle arrest. This is distinct from many of the more conventional chemotherapeutic agents that often focus on the cell cycle [41]. The modest S phase accumulation observed might still be beneficial when considering combination therapies, as it could potentially enhance the effects of S phase-specific agents like topoisomerase inhibitors or antimetabolites [42]. However, such combinations would need careful evaluation given that the cell cycle effects are not the dominant mechanism of action.

Comprehensive visualization of how water extract and VCA affect multiple cellular parameters simultaneously was defined by the heatmap analysis. We first show that, although both agents caused cell death, they induced significantly stronger caspase activation (>3 fold \log_2 change) by VCA compared to water extract, thus implying that VCA could be the main active component inducing apoptosis. Second, we observe minimal alterations in cell cycle-related parameters (generally <0.5 -fold \log_2 change) consistent with a significant cell cycle arrest observed upon activation of apoptotic programs, in line with our interpretation that both agents primarily act on the apoptotic machinery rather than through disruption of the cell cycle. Thus, these agents may principally cause cell death via the activation of direct apoptotic pathways, which is not consistent with the predominant effect of most conventional anticancer drugs, which primarily target the cell cycle [43]. This distinctive mode of action might be advantageous in treating cancer cells that have developed resistance to cell cycle-targeting drugs. Third, the differential responses between B16BL6 and B16F10 cells, particularly in their sensitivity to VCA-induced caspase activation, might be related to their different metastatic properties and could have implications for targeting different stages of melanoma progression.

Also, the multiparametric PCA revealed distinct clustering patterns between water extract and VCA treatments, suggesting different mechanistic pathways despite their common origin [44,45]. This analysis evaluates both cell viability and markers of apoptosis and cell cycle parameters, thus offering a holistic picture of the differential cellular response to these treatments that would support the complementary therapeutics applications of these treatments. Additionally, the correlation analysis provided insights into the relationships between different cellular responses to mistletoe extract and VCA treatment. B16BL6 cells showed a strong negative correlation between cell viability and total caspase activity ($r = -0.843$), while B16F10 cells exhibited a slightly stronger correlation ($r = -0.878$). The stronger correlations between early apoptosis and caspase markers in B16F10 cells ($r = 0.912$) compared to B16BL6 cells suggest potential cell line-specific differences in the timing or mechanism of apoptosis activation. Consequently, these findings corroborate with other studies that have demonstrated that the same stimulus elicits different apoptotic responses in different melanoma cell lines [46].

The hierarchical clustering analysis provides important insights into the differential responses of B16BL6 and B16F10 melanoma cells to Korean mistletoe water extract and its lectin. The clustering patterns suggest that at lower concentrations, the cellular responses are predominantly cell line-specific, possibly reflecting inherent differences in the molecular characteristics of these cell lines. However, at high concentrations, both treatments induce similar response patterns across cell lines, suggesting the activation of common cell death mechanisms. Treatment with medium concentrations tested (100 $\mu\text{g}/\text{mL}$ water extract and 0.1 $\mu\text{g}/\text{mL}$ VCA) clustered more closely to each other within the range of each cell line, suggesting that these concentrations

may represent a threshold at which significant cellular responses occur. The distinct clustering of high-concentration treatments suggests that the doses might overcome cell line-specific differences through the activation of universal apoptotic pathways [47,48].

Our integration analysis revealed distinct mechanisms of action between mistletoe water extract and VCA in melanoma cells. The water extract demonstrated a pattern consistent with prior reports of plant-derived compounds which may induce G0/G1 arrest before induction of apoptosis in cancer cells [49]. However, VCA induced strong apoptosis in the absence of significant G0/G1 arrest, similar to the known activities of other plant lectins, which can directly activate demise receptor pathways [50]. These findings indicate that the synergistic actions of various components of mistletoe collectively mediate its overall anticancer effects. To provide a standardized measure of treatment impact independent of treatment and reactor parameters, an effect size analysis was conducted, enabling water extract and VCA effects to be directly compared. The large effect sizes observed for cell viability and apoptotic markers even at moderate concentrations suggest that both treatments are highly effective in targeting melanoma cells. The gradual increase in effect sizes with concentration demonstrates a clear dose-response relationship. Notably, VCA showed comparable or larger effect sizes than water extract at lower concentrations (ng/mL vs. µg/mL), indicating its higher potency.

Further investigations need to be conducted to understand the molecular mechanisms involved in the observed effects, particularly focusing on the direct activation of caspase cascades and apoptotic signaling pathways. Additionally, studying the potential effects on upstream regulators of apoptosis, such as Bcl-2 family proteins and death receptors, may better explain the mechanism through which these agents induce their potent pro-apoptotic effects while minimally affecting cell cycle progression. Given the differential responses observed between primary and metastatic melanoma cell lines, future studies should investigate the potential anti-metastatic properties and underlying mechanisms, particularly focusing on EMT markers and invasion-related pathways. Moreover, considering the potent effects of VCA at nanogram concentrations, further investigation into the synergistic potential of combining VCA with conventional chemotherapeutics could provide valuable insights for clinical applications in melanoma treatment.

5 Conclusion

This study demonstrates that VCA exhibits potent anticancer effects against both primary and metastatic melanoma cells through distinct mechanisms. VCA showed particularly strong effects at nanogram concentrations, primarily through activation of caspase-dependent apoptotic pathways, while the water extract showed broader effects including modest cell cycle modulation. Multiparameter analysis revealed that both agents induce strong apoptotic responses with minimal impact on cell cycle progression, suggesting their potential as complementary therapeutic agents for melanoma treatment. The differential responses between B16BL6 and B16F10 cells also indicate possible cell-type specific mechanisms that warrant further investigation. These findings provide a comprehensive foundation for developing novel natural product-based strategies against aggressive melanoma, particularly highlighting the potential of VCA as a potent anticancer agent.

Acknowledgement: None.

Funding Statement: The authors received no specific funding for this study.

Author Contributions: The authors confirm contribution to the paper as follows: study conception and design: Chang-Eui Hong and Su-Yun Lyu; data collection: Chang-Eui Hong; analysis and interpretation of results: Chang-Eui Hong and Su-Yun Lyu; draft manuscript preparation: Chang-Eui Hong and Su-Yun Lyu. All authors reviewed the results and approved the final version of the manuscript.

Availability of Data and Materials: The datasets generated and/or analyzed during the current study are available from the corresponding author on reasonable request.

Ethics Approval: Not applicable.

Conflicts of Interest: The authors declare no conflicts of interest to report regarding the present study.

Appendix A

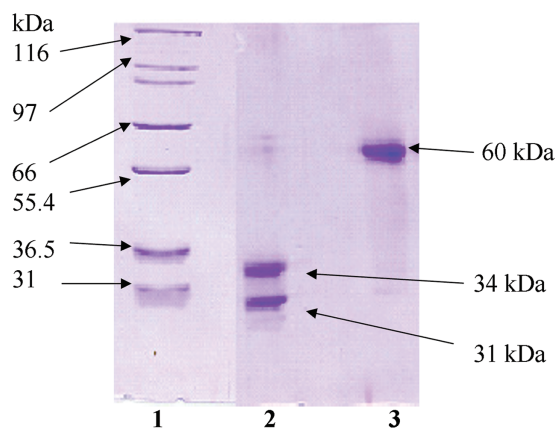


Figure A1: Electrophoretic characterization of *Viscum album* L. var. *coloratum* agglutinin (VCA) under different conditions. Protein fractions obtained through sequential purification using SP-50 Sephadex C-50 followed by asialofetuin-Sepharose 4B chromatography were subjected to SDS-PAGE analysis. Migration patterns were examined with (lane 2) and without (lane 3) reductive conditions. Reference molecular mass standards are shown in lane 1

References

1. Siegel RL, Miller KD, Fuchs HE, Jemal A. Cancer statistics, 2021. *CA Cancer J Clin.* 2021;71(1):7–33. doi:10.3322/caac.21654.
2. Bray F, Laversanne M, Sung H, Ferlay J, Siegel RL, Soerjomataram I et al. Global cancer statistics 2022: GLOBOCAN estimates of incidence and mortality worldwide for 36 cancers in 185 countries. *CA Cancer J Clin.* 2024;74(3):229–63. doi:10.3322/caac.21834.
3. Wang S, Liu C, Yang C, Jin Y, Cui Q, Wang D, et al. PI3K/AKT/mTOR and PD-1/CTLA-4/CD28 pathways as key targets of cancer immunotherapy (Review). *Oncol Lett.* 2024;28(6):567. doi:10.3892/ol.2024.14700.
4. Diaz LA, Cantley LC. The hallmarks of a cancer discovery. *Cancer Discov.* 2023;13(4):797–8. doi:10.1158/2159-8290.CD-23-0171.
5. Hartman ML, Czyz M. Anti-apoptotic proteins on guard of melanoma cell survival. *Cancer Lett.* 2013;331(1):24–34. doi:10.1016/j.canlet.2013.01.010.
6. Hart IR. The selection and characterization of an invasive variant of the B16 melanoma. *Am J Pathol.* 1979;97(3):587–600.
7. Fidler IJ. Selection of successive tumour lines for metastasis. *Nat New Biol.* 1973;242(118):148–9. doi:10.1038/newbio242148a0.
8. Koochaki R, Amini E, Zarehossini S, Zareh D, Haftcheshmeh SM, Jha SK et al. Alkaloids in cancer therapy: targeting the tumor microenvironment and metastasis signaling pathways. *Fitoterapia.* 2024;179:106222. doi:10.1016/j.fitote.2024.106222.
9. Hong CE, Lyu SY. Modulation of breast cancer cell apoptosis and macrophage polarization by mistletoe lectin in 2D and 3D models. *Int J Mol Sci.* 2024;25(15):8459. doi:10.3390/ijms25158459.

10. Khil LY, Kim W, Lyu S, Park WB, Yoon JW, Jun HS. Mechanisms involved in Korean mistletoe lectin-induced apoptosis of cancer cells. *World J Gastroenterol.* 2007;13(20):2811–8. doi:10.3748/wjg.v13.i20.2811.
11. Lyu SY, Park WB. Mistletoe lectin modulates intestinal epithelial cell-derived cytokines and B cell IgA secretion. *Arch Pharm Res.* 2009;32(3):443–51. doi:10.1007/s12272-009-1319-6.
12. Griffioen AW, Nowak-Sliwinska P. Programmed cell death lives. *Apoptosis.* 2022;27(9–10):619–21. doi:10.1007/s10495-022-01758-5.
13. Weeks AM. Kinases leave their mark on caspase substrates. *Biochem J.* 2021;478(17):3179–84. doi:10.1042/BCJ20210399.
14. Han JH, Tweedell RE, Kanneganti TD. Evaluation of caspase activation to assess innate immune cell death. *J Vis Exp.* 2023;(191):e64308. doi:10.3791/64308.
15. Tiwari SK, Sivasailam A, Maliakkal RT, Pillai PR, Surabhi SV, Prasad T, et al. Quantitative analysis of apoptosis and necrosis in live cells using flow cytometry. *Methods Mol Biol.* 2022;2543:57–69. doi:10.1007/978-1-0716-2553-8.
16. Niles AL, Kupcho KR. A nondestructive, real-time Annexin V apoptosis assay. *Methods Mol Biol.* 2022;2543:1–11. doi:10.1007/978-1-0716-2553-8.
17. Petroni G, Formenti SC, Chen-Kiang S, Galluzzi L. Immunomodulation by anticancer cell cycle inhibitors. *Nat Rev Immunol.* 2020;20(11):669–79. doi:10.1038/s41577-020-0300-y.
18. Ma L, Jiang Z, Hou X, Xu Y, Chen Z, Zhang S, et al. LA-D-B1, a novel Abemaciclib derivative, exerts anti-breast cancer effects through CDK4/6. *BIOCELL.* 2024;48(5):847–60. doi:10.32604/biocell.2024.050868.
19. Cech NB, Oberlies NH. From plant to cancer drug: lessons learned from the discovery of taxol. *Nat Prod Rep.* 2023;40(7):1153–7. doi:10.1039/D3NP00017F.
20. Schettini F, De Santo I, Rea CG, De Placido P, Formisano L, Giuliano M, et al. CDK 4/6 inhibitors as single agent in advanced solid tumors. *Front Oncol.* 2018;8:608. doi:10.3389/fonc.2018.00608.
21. Beck D, Niessner H, Smalley KS, Flaherty K, Paraiso KH, Busch C, et al. Vemurafenib potently induces endoplasmic reticulum stress-mediated apoptosis in BRAFV600E melanoma cells. *Sci Signal.* 2013;6(260):ra7. doi:10.1126/scisignal.2003057.
22. Darzynkiewicz Z, Crissman H, Jacobberger JW. Cytometry of the cell cycle: cycling through history. *Cytometry A.* 2004;58(1):21–32. doi:10.1002/cyto.a.20003.
23. Gu Z. Complex heatmap visualization. *Imeta.* 2022;1(3):e43. doi:10.1002/imt.243.
24. Kim J, Kim DH, Kwak SG. Comprehensive guidelines for appropriate statistical analysis methods in research. *Korean J Anesthesiol.* 2024;77(5):503–17. doi:10.4097/kja.24016.
25. Adzhiakhmetova SL, Chervonnaya NM, Pozdnyakov DI, Popova OI, Oganisyan ET. Component composition and features of biological activity of *Viscum album* (Viscaceae). *Dokl Biol Sci.* 2024;518(1):116–32. doi:10.1134/S0012496624701072.
26. Rajčević N, Bukvički D, Dodoš T, Marin PD. Interactions between natural products—a review. *Metabolites.* 2022;12(12):1256. doi:10.3390/metabo12121256.
27. Xie L, Wang J, Song L, Jiang T, Yan F. Cell-cycle dependent nuclear gene delivery enhances the effects of E-cadherin against tumor invasion and metastasis. *Signal Transduct Target Ther.* 2023;8(1):182. doi:10.1038/s41392-023-01398-4.
28. Büssing A, Bischof M, Hatzmann W, Bartsch F, Soto-Vera D, Fronk EM, et al. Prevention of surgery-induced suppression of granulocyte function by intravenous application of a fermented extract from *Viscum album* L. in breast cancer patients. *Anticancer Res.* 2005;25(6C):4753–7.
29. Kröz M, Kienle GS, Feder G, Kaveri S, Rosenzweig S. Mistletoe: from basic research to clinical outcomes in cancer and other indications. *Evid Based Complement Alternat Med.* 2014;2014:987527. doi:10.1155/2014/987527.
30. Szurpnicka A, Kowalczyk A, Szterk A. Biological activity of mistletoe: *in vitro* and *in vivo* studies and mechanisms of action. *Arch Pharm Res.* 2020;43(6):593–629. doi:10.1007/s12272-020-01247-w.
31. Piao BK, Wang YX, Xie GR, Mansmann U, Matthes H, Beuth J, et al. Impact of complementary mistletoe extract treatment on quality of life in breast, ovarian and non-small cell lung cancer patients. A prospective randomized controlled clinical trial. *Anticancer Res.* 2004;24(1):303–9.

32. Timis T, Bergthorsson JT, Greiff V, Cenariu M, Cenariu D. Pathology and molecular biology of melanoma. *Curr Issues Mol Biol.* 2023;45(7):5575–97. doi:10.3390/cimb45070352.
33. Liu QL, Luo M, Huang C, Chen HN, Zhou ZG. Epigenetic regulation of epithelial to mesenchymal transition in the cancer metastatic cascade: implications for cancer therapy. *Front Oncol.* 2021;11:657546. doi:10.3389/fonc.2021.657546.
34. Lyu SY, Park WB. Effects of Korean mistletoe lectin (*Viscum album coloratum*) on proliferation and cytokine expression in human peripheral blood mononuclear cells and T-lymphocytes. *Arch Pharm Res.* 2007;30(10):1252–64. doi:10.1007/BF02980266.
35. Amaral T, Sinnberg T, Meier F, Krepler C, Levesque M, Niessner H, et al. The mitogen-activated protein kinase pathway in melanoma part I—activation and primary resistance mechanisms to BRAF inhibition. *Eur J Cancer.* 2017;73:85–92. doi:10.1016/j.ejca.2016.12.010.
36. Wan Y, Liu T, Hou X, Dun Y, Guan P, Fang H. Antagonists of IAP proteins: novel anti-tumor agents. *Curr Med Chem.* 2014;21(34):3877–92. doi:10.2174/0929867321666140826115258.
37. Kubczak M, Szustka A, Rogalińska M. Molecular targets of natural compounds with anti-cancer properties. *Int J Mol Sci.* 2021;22(24):13659. doi:10.3390/ijms222413659.
38. Rajabi S, Maresca M, Yumashev AV, Choopani R, Hajimehdipoor H. The most competent plant-derived natural products for targeting apoptosis in cancer therapy. *Biomolecules.* 2021;11(4):534. doi:10.3390/biom11040534.
39. Zhang J, Wu Y, Li Y, Li S, Liu J, Yang X, et al. Natural products and derivatives for breast cancer treatment: from drug discovery to molecular mechanism. *Phytomedicine.* 2024;129:155600. doi:10.1016/j.phymed.2024.155600.
40. Zeman MK, Cimprich KA. Causes and consequences of replication stress. *Nat Cell Biol.* 2014;16(1):2–9. doi:10.1038/ncb2897.
41. Mostofa A, Punganuru SR, Madala HR, Srivenugopal KS. S-phase specific downregulation of human O⁶-Methylguanine DNA Methyltransferase (MGMT) and its serendipitous interactions with PCNA and p21^{cip1} proteins in glioma cells. *Neoplasia.* 2018;20(4):305–23. doi:10.1016/j.neo.2018.01.010.
42. Kleinsimon S, Kauczor G, Jaeger S, Eggert A, Seifert G, Delebinski C. *Viscum*TT induces apoptosis and alters IAP expression in osteosarcoma *in vitro* and has synergistic action when combined with different chemotherapeutic drugs. *BMC Complement Altern Med.* 2017;17(1):26. doi:10.1186/s12906-016-1545-7.
43. Evan GI, Vousden KH. Proliferation, cell cycle and apoptosis in cancer. *Nature.* 2001;411(6835):342–8. doi:10.1038/35077213.
44. Jung ML, Baudino S, Ribéreau-Gayon G, Beck JP. Characterization of cytotoxic proteins from mistletoe (*Viscum album* L.). *Cancer Lett.* 1990;51(2):103–8. doi:10.1016/0304-3835(90)90044-x.
45. Choi SH, Lyu SY, Park WB. Mistletoe lectin induces apoptosis and telomerase inhibition in human A253 cancer cells through dephosphorylation of Akt. *Arch Pharm Res.* 2004;27(1):68–76. doi:10.1007/bf02980049.
46. Hsieh MY, Hsu SK, Liu TY, Wu CY, Chiu CC. Melanoma biology and treatment: a review of novel regulated cell death-based approaches. *Cancer Cell Int.* 2024;24(1):63. doi:10.1186/s12935-024-03220-9.
47. Melo-Lima S, Celeste Lopes M, Mollinedo F. Necroptosis is associated with low procaspase-8 and active RIPK1 and -3 in human glioma cells. *Oncoscience.* 2014;1(10):649–64. doi:10.18632/oncoscience.89.
48. Ryu K, Susa M, Choy E, Yang C, Hornicek FJ, Mankin HJ et al. Oleanane triterpenoid CDDO-Me induces apoptosis in multidrug resistant osteosarcoma cells through inhibition of Stat3 pathway. *BMC Cancer.* 2010;10:187. doi:10.1186/1471-2407-10-187.
49. Bailon-Moscoso N, Cevallos-Solorzano G, Romero-Benavides JC, Orellana MI. Natural compounds as modulators of cell cycle arrest: application for anticancer chemotherapies. *Curr Genomics.* 2017;18(2):106–31. doi:10.2174/1389202917666160808125645.
50. Mazalovska M, Kouokam JC. Plant-derived lectins as potential cancer therapeutics and diagnostic tools. *Biomed Res Int.* 2020;2020:1631394. doi:10.1155/2020/1631394.